Lund University

LUNDS UNIVERSITET

Faculty of engineering - Department of Solid State Physics

AlP sacrificial layer for GaP NW growth

A thesis submitted for the degree of Master of Nanoscience

Author:
Patrick Flatt

Faculty supervisors:
Prof. Magnus Borgström
M.Sc. Lukas Hrachowina

Faculty Opponent:
Assoc. Prof. Carina Fasth

Supervisor at AligND AB:
M.Sc. Niklas Mårtensson

June 2020

AlP sacrificial layer for GaP NW growth

By: Patrick Flatt

Abstract

III-V semiconductor nanowires (NWs) display outstanding potential for many technological applications, but their implementation into devices is restricted due to high material and fabrication costs. Common techniques for NW synthesis rely on single crystalline substrates, which are single-use and have large costs associated to them.

In this project a method for substrate reuse was designed and investigated. An aluminum phosphide (AlP) segment was grown as the base of gallium phosphide (GaP) NWs. The AlP segment was used as a sacrificial layer, allowing for separation of the GaP NWs from the GaP substrates used, thereby allowing for several uses of a substrate. These axial AlP/-GaP NWs were synthesized with the vapor-liquid-solid growth mode, using metal organic vapor phase epitaxy. During the project, the combination of the AlP and GaP compound materials was investigated regarding epitaxial growth, chemical etch characteristics and potential for substrate reuse.

As a reference to the approach with an AlP sacrificial layer it was investigated if reuse of a GaP wafer was possible after standard GaP NW growth. The wafer surface was planarized by wet chemical etching, before processing was performed. Regrowth of GaP NWs was possible with a yield of 50 %.

The highest yields obtained for GaP, AlP and axial AlP/GaP NW growth were 96 %, 96 % and 97 % respectively. For the regrowth experiments axial AlP/GaP NWs were grown with a 80 % yield on 1×1 cm^2 substrates. This project reports on two cycles of reuse using this approach. For the first cycle an overall yield of 82 % could be achieved, during the given time of this project, and in the second cycle the yield was slightly lower at 75 %. The substrates were still intact after the second regrowth and it should be possible to further reuse them.

KEYWORDS: *Nanowire, Substrate Reuse, Sacrificial Layer, Epitaxy, Wafer, MOVPE, Etching, GaP, AlP, SiN, Au, SEM*

Acknowledgements

First I would like to thank Lukas Hrachowina for all the guidance and support he gave me during the project. I am extremely grateful that he was my laboratory supervisor. He was an excellent teacher, being patient and always available to help. I have learnt a lot from him and wish him nothing but the best.

I would also like to express gratitude toward Magnus Borgström, Erik Smith, Niklas Mårtensson and Jaime Castillo-León for giving me the opportunity to write my thesis in a collaboration between Lund University, department of Solid State Physics, and the company AligND Systems. Magnus, who is an expert in the field of Nanoscience and Nanowire growth, was an invaluable asset for the project and took his time to help me in many situations. Niklas guided and introduced me to the industrial side of Nanotechnology.

The Epi group, which I took part in during the project work, was very welcoming. The valuable discussions we had helped me, as well as my thesis work, significantly. The group gave me fresh ideas and feedback on my laboratory work, and shared their experiences. Part of the group; David Alcer and Enrique Barrigón, also helped me with processing of the wafers.

A big thanks to Reza Jafari Jam for contributing to this project with his expertise and knowledge in the field of nanoprocessing. I am very grateful that he put in the time and effort to help with the electroplating of the samples.

I would like to thank Sungyoun Ju and Peter Blomqvist for working hard to assure that all hardware in the lab was up and running. Without their extra efforts it would not been possible for me to finish my thesis on time.

Last but not least, I would like to thank my family, girlfriend and friends for all the help and support during the time of this project. It has made the journey easier and more enjoyable.

Recycling in Nanotechnology

As technology advances, components in devices become smaller. A promising candidate for many applications are nanowires (NWs). NWs are tiny and needle like, meaning they are small in one dimension and more than thousand time larger in the other. If their feature sizes are compared to a human hair, it would be possible to fit thousands of these devices across the thickness of a single hair strand.

Nanotechnology based on NWs and new materials offer promising capabilities compared to conventional techniques. Applications include optical devices, where NWs can be used to more efficiently emit, guide and concentrate light. Although this new technology holds promising capabilities it is to date not commonly utilized in devices, since material and fabrication costs are much higher than for conventional techniques.

NWs can be produced in many different ways. One of the most common techniques involves growth of NWs from seed particles that are placed on a large surface, or substrate. This substrate acts as template for the growing NWs. NW growth functions similarly to how plants grow, where the seed particle is provided with nutrients and energy to grow. The substrates on which the NWs grow, are typically only used once, highly expensive and rare, therefore limiting this approach.

In this project we present and investigate a new method, that allows for multiple use of such expensive substrates. The method allows the substrates to be in a constant NW production cycle, where the NWs are removed and used as building blocks in devices. The approach involves the growth of a new material combination, where one material has the characteristic of being very easily removed by chemicals. For a visual representation of the method see figure 1.

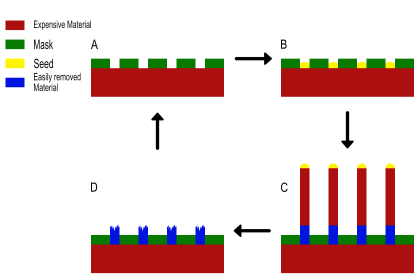

(a) Schematic of the sample cross-section.

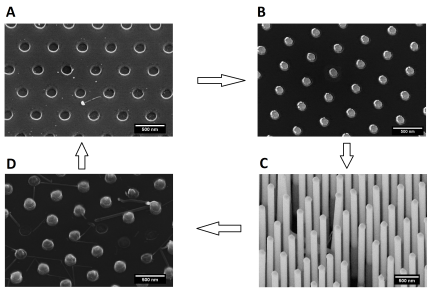

(b) Representational images from this work. Imaged at 30° tilt.

Figure 1: Shows the approach designed and used in this project for substrate reuse. A. Substrate to be reused. B. Seed particles. C. NWs. D. Residues.

Nomenclature

AlP Aluminium Phosphide

Au Gold

BARC Bottom Anti-Reflection Coating

CMP Chemical Mechanical Polishing

DI Deionized

DTL Displacement Talbot Lithography

DUV Deep-Ultraviolet

ELO Epitaxial Lift-Off

GaP Gallium Phosphide

H_2O Water

HCl Hydrochloric acid

HNO_3 Nitric acid

LOR Lift Off Resist

MOVPE Metalorganic Vapour-Phase Epitaxy

NW Nanowire

PE-CVD Plasma-Enhanced Chemical Vapour Deposition

PH_3 Phosphine

RF Radio Frequency

RIE Reactive Ion Etching

SEM Scanning Electron Microscope

Si Silicon

SiN Silicon Nitride

TMAl Trimethylaluminum, $Al_2(CH_3)_6$

TMGa Trimethylgallium, $Ga(CH_3)_3$

TMIn Trimethylindium, $In(CH_3)_3$

VLS Vapor-Liquid-Solid

XEDS Energy-dispersive X-ray spectroscopy

Contents

1 Introduction **9**
- 1.1 Motivation of Thesis . . . 10
- 1.2 Background . . . 10
  - 1.2.1 Substrate Reuse . . . 11
  - 1.2.2 Theory of MOVPE and VLS-growth . . . 13

2 Methodology **18**
- 2.1 Substrates . . . 18
  - 2.1.1 Pre-Processing . . . 19
- 2.2 Wafer Processing . . . 20
  - 2.2.1 Mask Deposition . . . 21
  - 2.2.2 Lithography . . . 21
  - 2.2.3 Pattern Transfer . . . 21
  - 2.2.4 Seed Particle Deposition . . . 22
  - 2.2.5 Wafer Dicing . . . 22
- 2.3 NW Growth Optimization . . . 23
  - 2.3.1 Etch and Cover Run . . . 23
  - 2.3.2 Growth Recipes . . . 23
  - 2.3.3 Growth Characterization . . . 24
- 2.4 Etch Characterization . . . 24
  - 2.4.1 GaP NW Etch . . . 24
  - 2.4.2 AlP Etch . . . 25
- 2.5 Substrate Reuse . . . 25

3 Results and Discussion **26**
- 3.1 Pre-Processing . . . 26
  - 3.1.1 GaP Surface Planarization . . . 26
- 3.2 Wafer Processing . . . 28
- 3.3 Growth Optimization . . . 31
  - 3.3.1 GaP NW Growth . . . 31
  - 3.3.2 AlP NW Growth . . . 34
  - 3.3.3 The Substrates Effect on Growth . . . 39
  - 3.3.4 Axial AlP/GaP NW Growth . . . 41

3.4 Etching Characterization 43
3.4.1 GaP Etch 43
3.4.2 AlP Etch 46
3.5 Substrate Reuse without Sacrificial Layer 49
3.6 Substrate Reuse with Sacrificial Layer 50
3.6.1 NW Growth 50
3.6.2 Substrate Preparation for Regrowth 53
3.6.3 Regrowth 57
3.6.4 Second Reuse 60

4 Conclusions **63**
4.1 Outlook 64

A Theory of processing techniques **66**
A.1 Plasma-Enhanced Chemical Vapour Deposition 66
A.2 Displacement Talbot Lithography 67
A.3 Reactive Ion Etching 68
A.4 Thermal Evaporation 69
A.5 Lift-Off 70
A.6 Pulsed Electrodeposition 71

B Experimental Details **74**
B.1 Substrate Preparation Before Processing 74
B.1.1 Substrate Cleaning 74
B.1.2 GaP Wafer Etch 74
B.2 Wafer Processing 75
B.2.1 Mask Deposition 75
B.2.2 Lithography 75
B.2.3 Pattern Transfer 76
B.2.4 Seed Particle Deposition 77
B.2.5 Wafer Dicing 77
B.3 NW Growth Optimization 78
B.3.1 Etch and Cover run 78
B.3.2 The Structure of the Growth Recipes 78
B.3.3 Growth Recipes 79
B.3.4 Growth Characterization 80
B.4 Etch Characterization 81
B.4.1 GaP NW Etch 81
B.4.2 AlP Etch 81
B.5 Substrate Reuse 81
B.5.1 Etching 81
B.5.2 Electroplating 82

Chapter 1

Introduction

Semiconductor nanowires (NWs) have in the recent years become a hot topic in the scientific community due to their unique properties and promising potentials for many applications [1, 2, 3]. Applications include photonics [4], energy technologies [5], sensors [6], transistors [7] etc. NWs are typically several micrometers long with a diameter on the nanoscale, needle like, and can be made from many different materials and material combinations, such as the III-V semiconductors [8].

Producing NWs through metal organic vapour phase epitaxy (MOVPE) from seed particles gives NWs with high material quality and well controlled structural, electrical and optical qualities. The process is however limited regarding scale up with industrial production in mind, due to, in relation to other NW growth techniques, its high cost, the limited availability and cost of III-V substrates, low growth rate and it being a batch based process. [9, 10] For processes at the company AligND, the high material quality of the NWs are of importance and therefore a batch based process is still suitable, but production costs must be reduced.

The idea of this project work is to recycle the expensive single crystalline substrates used for epitaxial growth in MOVPE, thereby reducing costs significantly. By using the same substrate for NW growth several times, the substrate would also be in a constant production cycle of NW growth and removal, still being a batch based process, but being more efficient and economically favorable.

The approach we propose is to grow and mechanically remove axial AlP/GaP NWs from the substrate and thereafter, by selective wet chemical etching of AlP residues and electroplating, prepare the substrates for regrowth. Combining this process with the alignment technology available at AligND Systems, which can be used to vertically order the GaP NWs

on desired substrates, allows for further processing of the NWs and eventually use in devices. The major benefit of the sacrificial layer and selective etching is that it would theoretically be possible to indefinitely reuse the wafer.

If it is possible to reliably synthesise GaP NWs using this technique, final costs of devices based on GaP NWs would decrease dramatically. This decrease in cost could lead to that GaP NWs could be used in more applications and make them more available. The same methodology might also be applicable on other III-V semiconductor NWs with the same or different sacrificial layers.

1.1 Motivation of Thesis

This project will further and allow more research and industrial adaptation of III-V semiconductor systems. The project will help to understand and utilize these systems promising capabilities to a further extent than what is possible today. By reducing the production costs of III-V material NWs their availability and practical applications could increase.

Similar studies have been performed, with limited success. This study will carry novelty since the approach to use the elemental combination AlP/GaP has not yet been investigated in the growth of axial AlP/GaP NWs or in regard to substrate reuse. Also AlP is not extensively studied, neither in thin film nor NW technologies, and therefore any findings in this study could increase the understanding of the material.

This project will give insight into growth processes, material properties and interfaces, etching properties, potential for substrate reuse and more of axial AlP/GaP NWs. It will contribute to the understanding in areas such as physics, chemistry and material science.

1.2 Background

In this section the fundamental principles of substrate reuse will be described, as well as NW growth with MOVPE. Before the approach developed in this project is described, previous work in the field of substrate reuse is introduced. To give insight into crystal growth we describe the MOVPE process, first in general, then in more detail regarding reactions and mechanisms. Lastly the VLS mechanism for NW growth with MOVPE

is described. For the basic theory of the various processing techniques used in this project, view Appendix A.

1.2.1 Substrate Reuse

Previous Work

Currently reuse of III-V substrates is very limited, and definitely not a standard. A widely known technique in thin film technologies that has been reported on is epitaxial lift-off (ELO) [11, 12]. In the article from G. J. Bauhuis et. al [12] it has been shown possible to reuse a gallium arsenide (GaAs) substrate twice with ELO using an aluminum arsenide (AlAs) layer as lift-off layer, also called sacrificial layer. However after the ELO, a chemical mechanical polishing (CMP) process was required for the substrate reuse, and even with CMP the reuse resulted in reduced efficiency of the final device produced.

Any approach involving removal of substrate material is inefficient since the substrates then only can be reused very limited because of the decreasing thickness of the substrate. Altering thickness of the substrate after every reuse cycle could also affect processes, and thinner substrates become more brittle and harder to work with. [12]

Attempts have been made by R. J. Jam [13] to implement the thin film technology described above, from [12], into NW technology. His work was an inspiration to this project. In the article it was investigated if substrate reuse could be enabled by growing axial AlAs/GaAs NWs, synthesised by MOVPE. The approach R. J. Jam presents involves a SiN template mask that was used to define the position of the Au seed particles used for growth of the NWs. In the article one cycle of reuse at reduced yield is presented.

The largest problem faced in the article were that the SiN template mask delaminated from the substrates due to thermal stresses when working at high temperatures in the MOVPE reactor, requiring growth to occur at low temperatures. This made it unattainable to nucleate AlAs directly on GaAs, and therefore they had to nucleate the substrate material first before growing the sacrificial layer. This caused the growth of a GaAs stub that was becoming longer for every NW growth. This GaAs stub was making redefinition of the seed particles difficult and heavily limited the potential of regrowth.

Our Approach

We propose a new approach for substrate reuse, based on growing axial AlP/GaP NWs, where the AlP base is used as sacrificial layer. This approach could possibly also be used for other, similar material combinations, such as AlP/InP. Similar to R. J. Jams work, our method used requires processing of the bare wafers to prepare them for growth and reuse. First the substrates need to be covered with a SiN mask, which acts as a thermodynamically stable and chemically inert insulating layer. We expect to have less issues with the SiN mask at elevated temperatures than experienced in R. J. Jams work, since the Coefficient of Thermal Expansion (CTE) of GaP is closer to non stoichiometric thin film SiN, than that of GaAs [14, 15]. After deposition of the mask it is patterned with a hexagonal pattern of circular holes, that define the position of the Au seed particles.

The approach of substrate reuse by using a sacrificial layer is based on four steps, see figure 1.1.

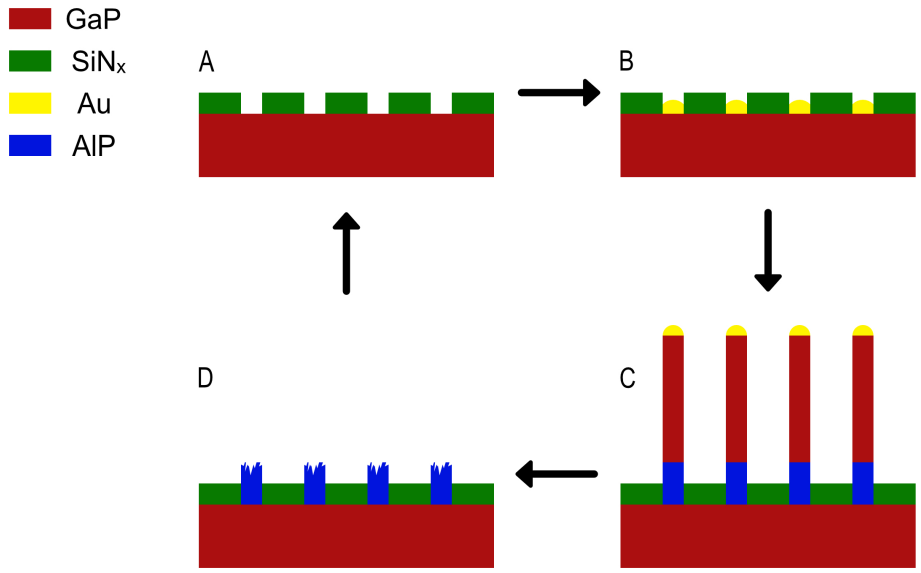

Figure 1.1: Shows a schematic of GaP NW synthesis by substrate reuse enabled by an AlP sacrificial layer. (A) The wafer and mask after processing or alternatively after selective wet chemical etching of AlP. (B) After seed particle definition. (C) After NW growth. (D) After NW harvesting.

First the Au seed particles for NW growth are defined inside the holes of the SiN mask, thereafter the axial AlP/GaP hetero NWs are grown using MOVPE. After growth the NWs are harvested by mechanical removal

from the substrate, leaving residues of AlP in the holes of the SiN mask. By selective wet chemical etching of the substrate all residues are removed, thereby returning the substrate to its original configuration, as before seed particle definition.

The major advantage of this approach is the selective etching of the sacrificial layer, theoretically enabling many cycles of reuse without affecting the substrate or the mask. The material combination of AlP/GaP has not been investigated in axial NW growth. The material combination has so far, in the regard of NW growth, only been investigated by M. T. Borgström et. al. [16], that showed that it is possible to grow AlP NWs on a GaP substrate. In the article radial core-shell AlP/GaP NWs were investigated. Their approach, similar to R. J. Jams work [13], included the nucleation of substrate material before growth of AlP NWs, and therefore it still remains unclear if AlP can be directly nucleated on a GaP substrate.

1.2.2 Theory of MOVPE and VLS-growth

Crystal growth in general is a very complex process, and many of the processes that lead to crystal growth in MOVPE are not completely understood. The growth process is manly divided into mass transport and thermodynamic, kinetic and hydrodynamic processes [17], and will be described in detail later. First the MOVPE process in general is described, and then the crystal growth as well as the VLS approach for NW growth.

Metalorganic Vapor-Phase Epitaxy

MOVPE is a common technique used in micro and nano fabrication to deposit epitaxial thin films [18, 19] and to grow NWs [20, 21]. In MOVPE metalorganic precursors are used to deposit singlecrystalline materials onto single crystalline substrates. Materials include III-V, II-VI compound semiconductor materials [22, 23]. In this project we focus only on III-V materials and therefore only describe the growth for these materials. Common group-V precursors are different hydrides, while common group-III precursors are hydrocarbon ligand subsituted group III metals, often trimethyl- or triethyl- based compounds [17, 24].

The principle behind MOVPE growth is that gaseous group-III and -V precursors are transported into the reactor where they react in various ways and deposit material on a substrate. For reactions to take place the substrate is heated on a susceptor inside a cold wall flow chamber, called

the liner. The precursors are transported into the reactor through different lines. The precursors are gaseous, however only the group-V precursors are stored in gas phase. Contrarily group-III precursors are usually stored in either liquid or solid state, and are therefore kept in stainless steel containers called bubblers. Inside the bubblers the pressure is controlled and the temperature is controlled by a thermostatic bath around the bubbler. Temperature and pressure both affect the vapour pressure of the materials, determining how much of the precursors is in gas phase. The amount that is in gas-phase is transported/pushed out of the bubbler by a so called "push flow" of an inert carrier gas, such as hydrogen or nitrogen. [22, 24]

Once the precursors enter the reactor they will mix and in complex chains of chemical reactions react and deposit the compound semiconductor material. Any rest products from the reactions are volatile and are removed from the reactor by the gas flow. For a schematic of a MOVPE reactor see figure 1.2.

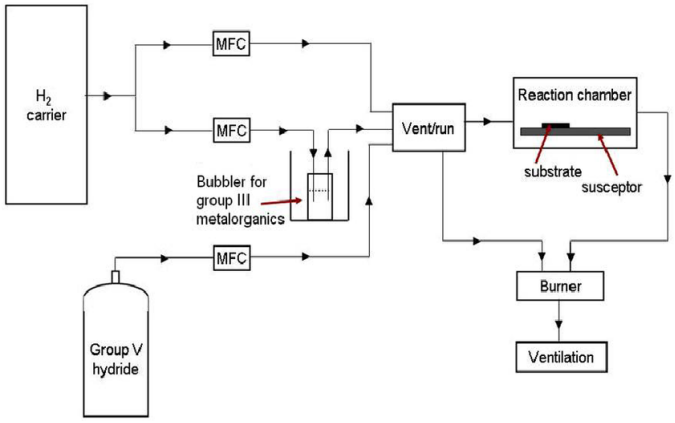

Figure 1.2: Shows a schematic of the fundamentals of a MOVPE reactor for growing III-V compound materials. The gaseous precursors are pushed into the reactor by an inert carrier gas, here hydrogen. The gas flow rates are controlled by mass flow controllers, MFC. In the reaction chamber the gases mix and undergo several reactions to deposit material on the hot substrate surface. Taken from [25].

Several processes occur after the precursors enter the reactor. The precursors enter the reactor through different lines, and will therefore first mix once they enter the reactor. After mixing some of the precursors immediately diffuse to the hot substrate surface where they react, others react first in gas phase before coming in contact with the heated substrate. The liner is not heated, but localized heating of only the substrate is not possible and therefore some parasitic reactions occur on the liner surface. If a completely clean liner is used this leads to quickly changing conditions in the reactor, therefore the liner has to be changed for every experiment.

This is a very time consuming process, and to avoid this typically an etch and cover run is used. Here the liner is coated in the material used for growth, and this leads to that parasitic reactions have a reduced effect on the conditions in the reactor. After the various reactions in the reactor the residues of the precursors are gaseous, and are flushed away by the gas flow.[22] For a schematic of the reactions see figure 1.3.

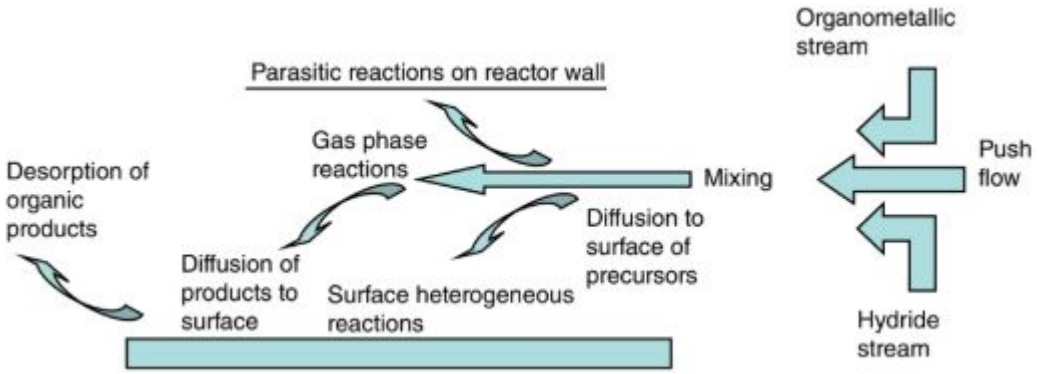

Figure 1.3: Shows a schematic of the various surface reactions during crystal growth in MOVPE. Taken from [22].

An important factor for crystal growth is the temperature used. In MOVPE different driving forces determine the rate of material deposition, depending on in which temperature regime the reactor is used. Usually the growth is divided into three main temperature regimes [22], as illustrated in figure 1.4.

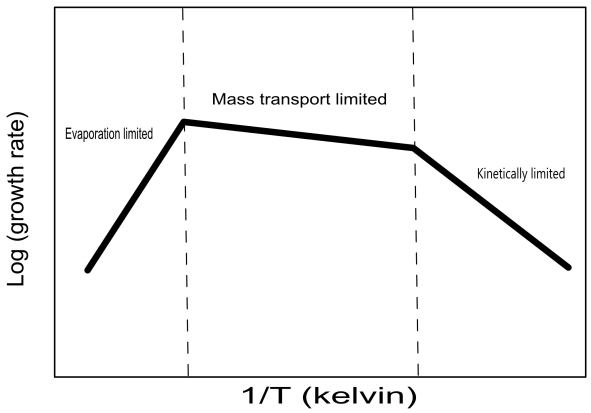

Figure 1.4: Shows a schematic of the three different growth regimes of MOVPE. The graph shows the effect of temperature on the growth rate.

At low temperatures growth is limited by the reaction rate of the precursors, the kinetics. At slightly higher temperatures the growth is instead limited by the amount of material that is provided to the vapor/solid interface, called mass transport. At even higher temperatures deposited growth species begin to evaporate from the solid surface and gas phase reactant depletion occurs, both reducing the amount of material that is deposited. It is often preferred to work in the transport limited regime due to it being easier to control growth rate, due to lower impact of temperature on growth rate.[22, 24]

Vapor-Liquid-Solid Mechanism

For NW growth in MOVPE the VLS growth mode is commonly used. In this growth technique it is used that crystal growth on a solid surface is very slow, while nanometer sized metal particles, called seed particles, act catalytic for deposition from vapor phase and thereby much more semiconductor material arrives at the seed particles compared to the substrate surface. Low temperatures can be used in VLS where growth on the substrate surface is kinetically limited, and therefore decreases drastically, and can also be completely suppressed. [26, 27, 28]

A common approach to grow III-V semiconductor NWs is to deposit the metal seed particles on (111) singlecrystalline substrates on which NWs, when grown epitaxially, grow perpendicular to the substrate surface [27]. The VLS approach enables growth of metastable crystal phases and heterostructures [29], even lattice-mismatched [30]. It also allows for fabrication of unusual ternary alloys and crystal phase tuning [31].

To initiate growth the precursors will dissolve in the seed particles and form a ternary alloy, that at the elevated temperatures results in a melt. When enough material is supplied from the vapor the droplet becomes supersaturated and material is deposited below the metal particle [27, 28]. However it is known that the solubility of group-V elements in liquid metals is low for most materials, it is therefore expected that most of the group-V elements diffuse in from the sides and nucleate at the triple phase line, just below the seed particle. This results in 2D nucleation below the seed particle, and thereby NW growth, as illustrated in figure 1.5.

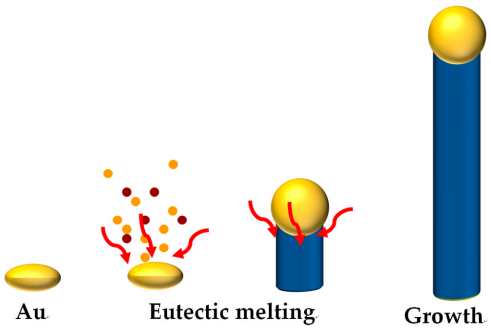

Figure 1.5: Shows a schematic of the VLS growth mode used to grow a NW. The Au seed particle acts as the preferred site of material deposition from the precursors. When enough material is dissolved in the particle it becomes supersaturated, resulting in that material deposits bellow the particle. Taken from [26].

The diameter of the grown NWs is mostly governed by the size of the seed particles, but can be tweaked by the growth conditions [27]. Other structural properties of the NWs, such as length, shape and crystal structure can also be tuned by the changing growth parameters such as temperature, V/III ratio and duration of the NW growth [27]. This is due to the thermodynamic parameters, volume and contact angle of the seed particle changing when becoming alloyed in different ways [27]. For example, it has been shown that NWs grown from smaller seed particles grow faster, and with higher crystal quality, than NWs from larger seed particles which grow slower with more defects and where kinking is more of a prominent issue. This is due to the higher solubility of group-III precursors and more efficient diffusion in the smaller particles. [32]

Another approach to control structural properties of the NWs is using *in situ* etching by HCl. The use of HCl not only affects the radial growth rates of the NWs and the contact angle of the seed particle, it is also believed to remove crystal defects and have an catalytic effect to the decomposition of the precursors. Its effects have been shown to improve the overall optical properties of NWs. [33]

Chapter 2

Methodology

In this chapter the methodology for the experimental work is introduced. Here every step is described, this includes; wafer processing, the optimization of NW growth, characterization of wet chemical etching of GaP and AlP, as well as the substrate reuse experiments.

Wafer processing describes the steps taken to prepare the wafers into the substrates later used for the NW growth. The section on NW growth optimization gives insight on how the NW growth recipes were designed. In the etch characterization the methods used to characterize the etching of AlP and GaP are shown. Lastly, the substrate reuse experiments are discussed. For the full details of the experimental work, see Appendix B.

2.1 Substrates

The wafers used during the entirety of the project were three S-doped (111)B GaP wafers, 2 inch (50.8 mm) with a thickness of 300 μm. The wafers were in different conditions when they were received. For convenience, they will be called wafer 1, 2 and 3 respectively. They are described by the list below.

1. Wafer 1
   This wafer was still sealed from the manufacturer, thereby being in the best condition possible. This wafer was used for the substrate reuse experiments enabled by a sacrificial layer of AlP, section 2.5.

2. Wafer 2
   Was exposed to a non clean room environment before processing. It therefore had to be cleaned before processing could begin. After cleaning, it should again be as new. It will be used for the optimization of the NW growth, section 2.3.

3. Wafer 3
   Had stubs of GaP on the surface from a previous GaP NW growth. The NWs had been grown using MOVPE and were removed by sonication. The wafer was used to investigate whether it is possible to perform epitaxial growth of GaP NWs on this substrate after surface planarization by chemical etching.

Si wafers were used during processing as dummy wafers to test processing steps before using the valuable GaP substrates.

2.1.1 Pre-Processing

Wafer 1 was ready for processing. Wafer 2 and 3 however had to be prepared with some pre-processing before the real processing could be started.

The wafer that was exposed to a non clean room environment, wafer 2, was cleaned with acetone and isopropanol, as in Appendix B.1.1, to assure that no contaminants were on the substrate surface that could impact processing.

Efforts were made to reuse wafer 3, on which GaP NWs had previously been grown. The NWs had already been removed by sonication, leaving stubs on the surface that we attempted to remove by wet chemical etching. Diluted aqua regia, $H_2O : HCl : HNO_3$, was mixed at a ratio of 3:3:2 and used as the etching solution. The wafer was etched twice for 5 minutes at 23 °C. Finally the wafer was etched for another 2 minutes at 45 °C using the same solution. After every etch cycle the wafer surface was visually inspected in SEM. The wafer surface was desired to be as flat as possible, without significant removal of bulk material.

2.2 Wafer Processing

Wafer processing includes all the steps that were taken to transfer the bare wafers into the substrates used for the experiments. The processing steps are illustrated in figure 2.1.

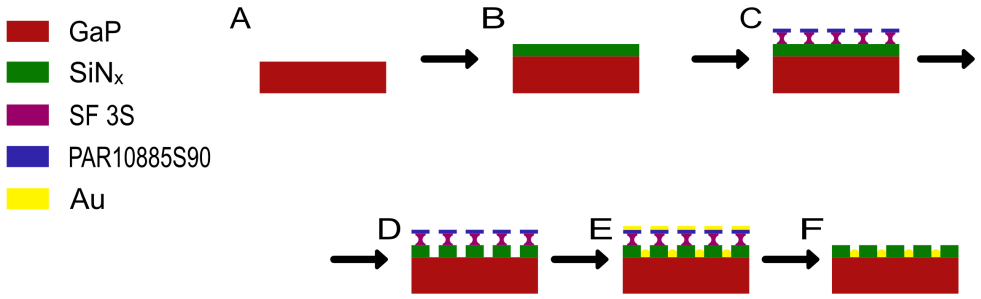

Figure 2.1: Shows a schematic of the processing, step-by-step. (A) Wafer before processing. (B) After mask deposition. (C) After lithography. (D) After pattern transfer. (E) After evaporation. (F) After lift-off.

The first processing step was to deposit a SiN mask on the wafers. Thereafter the nitride mask was covered with a double layer of resists, first a layer of bottom anti-reflection coating (BARC), SF 3S, and thereafter a layer of deep-ultraviolet (DUV) resist, PAR10885S90. The resists were used for pattern transfer into the SiN mask and seed particle definition. The nanopattern was first transferred into the resists by displacement talbot lithography and then into the SiN mask by reactive ion etching (RIE). The gold seed particles used for NW growth were defined using evaporation and lift-off.

The structure of the processing was the same for all three wafers, with only minor differences as described below, and in more detail in Appendix B.2.

2.2.1 Mask Deposition

The first process step was to deposit a 75 nm thick SiN mask. The SiN mask was deposited using a Micro Systems 200 ICP PE-CVD system. The CVD reactor was first loaded with a Si dummy wafer to ensure that all parameters were set correctly and to get an estimate of the deposition rate. After deposition on the dummy wafer, the thickness of the SiN layer was measured using ellipsometry and the deposition rate was calculated. Here, no changes were needed and the same process was repeated on the GaP wafer. The resulting thickness of the SiN layer on these wafers was also determined by ellipsometry since it is important for further processing steps. After this step the wafers were in the same state as in figure 2.1B.

2.2.2 Lithography

The first step to transfer the nanopattern into the SiN mask is the lithography. Here DTL was used with a PhableR 100 DUV system, capable of sub-100nm resolution. Before exposure the wafers were coated with two layers of developable resists. First a layer of a BARC, SF 3S, and then a layer of DUV resist, PAR1085S90. After applying the double-layer of resists, the wafer was exposed by DTL. To find an appropriate dose, two different exposure doses were tested on wafer 2. Half of the wafer was exposed with a dose of 3.0 mJ/cm^2 and the other half with 3.5 mJ/cm^2. The other two wafers, wafer 1 and 3, were exposed with a dose of 3.25 mJ/cm^2. After exposure by DTL the resists were developed in developer MF24A. The schematic in figure 2.1 shows the intended cross sectional profile of the layers after the developments of the resists.

2.2.3 Pattern Transfer

After lithography the nanopattern was transferred into the resist, but not into the SiN mask yet. For this RIE was used, which was carried out in a Sirus T2 Plus table-top RIE system. This etching process does not attack the resists used and leads to anisotropic etching of the SiN mask, hence only the exposed SiN below the openings in the resist will be etched.

The etch rate of the tool was drifting, hence a Si dummy wafer, prepared in the same way as all the wafers in section 2.1.1, was used to experimentally determine the etch rate. The thickness of the SiN on the dummy wafer was measured with ellipsometry before and after etching, giving an approximate etch rate of 0.3 nm/s. For the GaP wafers, wafer 1, 2 and 3, the time of the etch program was set to 233 seconds, therefore etching about 75 nm,

which corresponded to the thickness of the deposited SiN mask on the GaP wafers. Etching this exact amount enabled to etch all of the SiN without affecting the substrate. After the RIE the wafer was dipped in a diluted HF solution, HF:H_2O at a ratio of 1:100, to remove any residues of SiN in the holes of the SiN mask and to a much lesser extent the SiN growth mask.

After this process steps the SiN mask was patterned the same way as the resist was patterned by the DTL, so the pattern had been transferred into the SiN mask as in figure 2.1D.

2.2.4 Seed Particle Deposition

After the previous processing step, the patterning of the SiN mask by RIE, the gold seed particles were defined on the wafers. We did this by using evaporation followed by a lift-off procedure, which are standard techniques. However this was not optimal since electroplating would be used for the substrate reuse experiments. This was done since the electroplating had not been optimized for GaP, and use without optimization was to risky on wafer level. Instead electroplating was first used on, and optimized for, smaller substrate pieces during seed redefinition for substrate reuse.

For evaporation, a Temescal E-Beam evaporator, was set to deposit 65 nm of 24K gold, 99.95 % purity. Depositing this amount leaves approximately 10 nm room in the holes of the SiN mask to facilitate lift-off and growth. The same deposition was done on all three wafers.

Evaporation covered the entire surface of the wafers in gold, as in schematic figure 2.1E. To remove the excessive gold, which is on top of the resist, a lift-off using remover 1165 was performed. After lift-off there should only be gold inside the holes of the SiN mask, giving nicely defined seed particles for the NW growth that followed next. For a schematic of the substrate after finished processing see figure 2.1F.

2.2.5 Wafer Dicing

After the seed particle definition the wafers were divided into smaller substrates to suite different experiments.

The wafer for the reuse experiments, wafer 1, was diced in 1×1 cm^2 pieces with a Disco DAD 3320 dicer. This was done so that the samples would fit the holder for electroplating and also yield more material for use by AligND. The wafer used for the growth optimization, wafer 2, was broken into small pieces with a diamond tip pen. This was done to be able to

carry out many growth experiments on the limited substrate area, reducing material costs. The wafer planarized by chemical etching of the surface, wafer 3, was also divided by hand, but into larger pieces.

After these final steps all wafers were ready for NW growth. We started with growth optimization on wafer 2, described below.

2.3 NW Growth Optimization

After finished processing of the wafers it was proceeded with the first experiments of NW growth. Firstly recipes for the growth needed to be designed and tested. Substrates of wafer 2 were used to find the right growth conditions that later would be used for the experiments on wafer 1 and 3. We started with optimization of the GaP growth, then the AlP growth and lastly the growth of axial AlP/GaP NWs.

2.3.1 Etch and Cover Run

Before any NW growth was done the reactor was prepared. Before every experiment-session a fresh liner was placed in the reactor and a InP or GaP etch and cover run was performed. To grow GaP samples it is typical to use a GaP cover run, we began however with experiments in an InP cover run. This was done in an effort to work time efficient, since access to the reactor was limited, and other researchers experiments required the reactor to covered with In. The etch and cover runs used were previously known and not optimized. After the etch and cover run the reactor could be used to begin optimizing the growth recipes.

2.3.2 Growth Recipes

Growth recipes define the conditions that the samples are exposed to while being in the reactor; before, during and after growth. To grow NWs, the growth recipes needed to be optimized. For GaP this meant to test known recipes and adjust them to the specific MOVPE reactor used, an Aixtron 200/4. For the AlP and AlP/GaP growth completely new recipes were designed from ground up. The recipes were optimized by making changes to growth parameters, and observing their effects on growth. In this work adjustments were mostly made to the molar fractions of the different precursors used and durations of different steps of the growth recipes. For a fully detailed description of the recipes see Appendix B.3.

2.3.3 Growth Characterization

The NW growth was investigated *in-situ* by use of a custom built LayTec - Spectrum, as in [34]. After growth the NWs were thoroughly investigated in either a SEM - LEO 1560 Thermal Field Emission SEM or a Hitachi SU8010 Cold Field Emission SEM, depending on availability of the tools. LayTec was used to monitor NW length while the SEM images were analyzed, using the software ImageJ, to determine NW length more accurately as well as measuring diameters and quantifying the yield of the growth.

2.4 Etch Characterization

The purpose of this section is to evaluate the wet chemical etch characteristics of GaP and AlP NWs. To have insight into how materials and features etch is important to be able to controlled remove material. In the case of GaP surface planarization is of interest, removing GaP NW stubs while etching the substrate surface as little as possible. For AlP a selective etch is desired that efficiently removes AlP residues while not affecting the GaP substrate or the SiN mask of the samples.

2.4.1 GaP NW Etch

Previously to the surface planarization of wafer 3 by wet chemical etching, described in section 2.1.1, etching characteristics of GaP NWs were investigated. This was done to find the etching conditions that wafer 3 would be exposed to in order to remove GaP subs from its surface.

To evaluate the etch rate of GaP NWs, different etch durations and temperatures were investigated using small substrate pieces from the wafer used for growth optimization, wafer 2. These substrates had GaP NWs grown on them, as described in section 2.3. To determine the etch rate the diameter of the NWs was measured before and after etching. The diameters were measured at two areas of every NW, the top half as well as on the bottom half.

It should be noted that the samples used for these experiments had a SiN mask, covering the GaP surface of the substrate, however wafer 3 that would be etched had not. Therefore no etch characterization of the surface could be done on these substrates, only of the etch rate of the NWs.

2.4.2 AlP Etch

The etching experiments were carried out on samples having only AlP NWs, and no GaP segments. This was done to more easily be able to characterize the etching characteristics of the AlP. The etching solutions tested were DI-water, diluted HCl mixtures and a diluted piranha etch. Different solutions were tested to find the etching solution that later was used for the regrowth experiments, section 2.5. The purpose of the etching in the regrowth perspective is removing all AlP, clearing the holes of residues, without affecting the GaP surface bellow or the SiN mask. In a schematic it would be changing the substrate as in figure 1.1D to 1.1A.

2.5 Substrate Reuse

To test the potential of regrowth, axial AlP/GaP NWs were grown on the previously prepared 1×1 cm^2 substrates from wafer 1. The GaP segments of the NWs were harvested by AligND. Residues were then removed by etching the samples in $HCl : H_2O$ at a ratio of 1:1. After etching the substrates should again be in the state as in figure 1.1A.

To redefine the gold seed particles on the pieces from wafer 1, electroplating was used, where the insulating SiN mask acts as a template for the deposition. The set-up for the electroplating was based on a system from Yamamoto-MS, the same as in [13]. The electroplating was performed as in Appendix B.5.2.

After electroplating any organic residues that might had been deposited from the electrolyte solution had to be removed. This was done by an ozone cleaning process. Thereafter the substrates were ready for regrowth.

Chapter 3

Results and Discussion

In this chapter we present and discuss the findings made during this project. First the results of the Pre- and standard processing of the wafers are described, followed by GaP, AlP and axial AlP/GaP NW growth from the prepared substrates. After growth the etching characteristics of AlP and GaP were investigated and lastly we present the results of substrate reuse.

3.1 Pre-Processing

Cleaning of wafer 2 was standard procedure and no investigation of the wafer surface was done more than quick optical inspection, where the wafer showed to be clean. The results of the pre-processing of wafer 3 can be seen below.

3.1.1 GaP Surface Planarization

For the surface of wafer 3 before etching, see figure 3.1a. The etching with aqua regia, at room temperature, resulted in etching of certain facets as seen in figure 3.1b, which shows the wafer surface after a total of 10 minutes of etching. To force the etching into a more isotropic process, the temperature of the etchant was increased from 23 to 45 °C. With this temperature increase the etchant flattened the remaining facets of the NWs on the wafer after 2 more minutes of etching, see figure 3.1c.

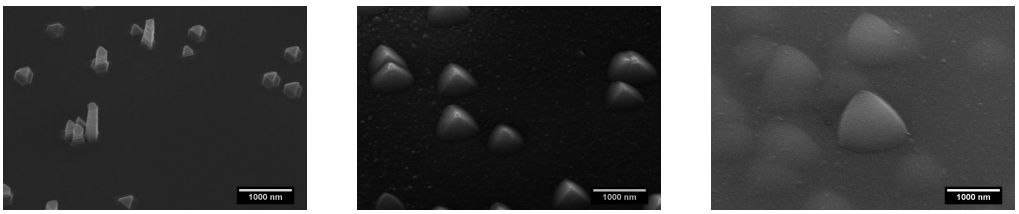

(a) Wafer surface before etching

(b) After 10 minute etch at 23 °C

(c) After another 2 minute etch at 45 °C

Figure 3.1: Shows representative images of the surface of wafer 3 at 30° tilt before and after different etching steps. The etchant used was $HCl : H_2O : HNO_3$ *at a ratio of 3:3:2.*

After etching at elevated temperature that the stubs could be flattened, however at the cost of a slightly more rough surface in general. The low temperature etch did not manage to etch certain facets efficiently. The (111) crystal planes etch the slowest in wet etching processes for crystals with the zinc blende structure [35, 36], which GaP crystallizes in [37]. The pyramids that are seen are probably (111)B planes, that previously have shown to etch faster in other etching solutions [38]. This is due to the crystallographic polarity of the zink blende structure and the surface energy being lower for the (111)B planes compared to other crystallographic directions [39].

It would have been desirable to use a low temperature etch since the etch rate is temperature dependent [40]. This is also the reason that lower temperatures were used, compared to previous experiments by M. T. Borgström et. al, where 80 °C were used [41]. The temperature increase from 23 to 45 °C showed to flatten the stubs much more efficiently. However, since a slightly rougher surface was observed in general after etching compared to an unused wafer it was decided not to proceed with any further etching. The attained results were deemed good enough to investigate if it is possible to grow from this reused substrate.

With these results in mind, it should be noted that the etching was not completely uniform over the entire surface of the 2" wafer. The area seen in figure 3.2 etched differently, showing a very rough profile. This occurred only locally and no similar area could be found on other parts of the wafer.

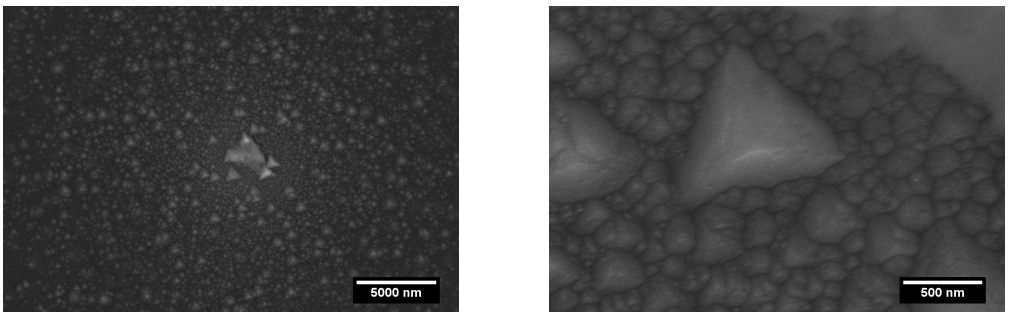

(a) Overview image *(b) Close-up image*

Figure 3.2: Shows top-view images of an area of the wafer that showed a vastly different etch profile than other areas, after the final etch.

Why the etching gave such a different result in this area of the wafer is unclear. Here facets of the remaining NWs were not etched completely, and the surface showed a very rough profile. This indicates that the etchant did not reach this area unhindered during the etching at elevated temperatures, perhaps gas bubbles formed and stayed at the liquid/solid interface from chemical reactions. Another explanation could be that the quality of the wafer in this area was worse and therefore responds differently to the etching. To avoid such issues it was made sure that the whole wafer was completely submerged during etching and the solution was stirred to further enhance homogeneous etching, but even with these precautions the etch was not completely homogeneous.

3.2 Wafer Processing

The results of the wafer processing are of importance since it can influence the NW growth and/or the reuse. The deposition of the SiN mask was set to 75 nm, and the resulting thicknesses were confirmed with ellipsometry to be 73.2, 74.9 and 72.6 nm for wafer 1, 2 and 3 respectively. After patterning by DTL, RIE and the HF-dipp, the average hole size in the nitride mask, and later the seed particle size, was 153, 161 and 175 nm for the Talbot exposure doses of 3.0, 3.25 and 3.5 mJ/cm^2 respectively. The height of the gold seed particles, deposited by thermal evaporation, was 65.3 nm on wafer 2 and 65.0 nm on wafer 1 and 3. The final results of processing on the different wafers look identical in SEM inspection, of course having differently sized seed particles, but regarding the pattern transfer and quality. There were a few exceptions however, which are discussed later. Representative images of the substrates after finished processing, ready for growth, are shown in figure 3.3 below.

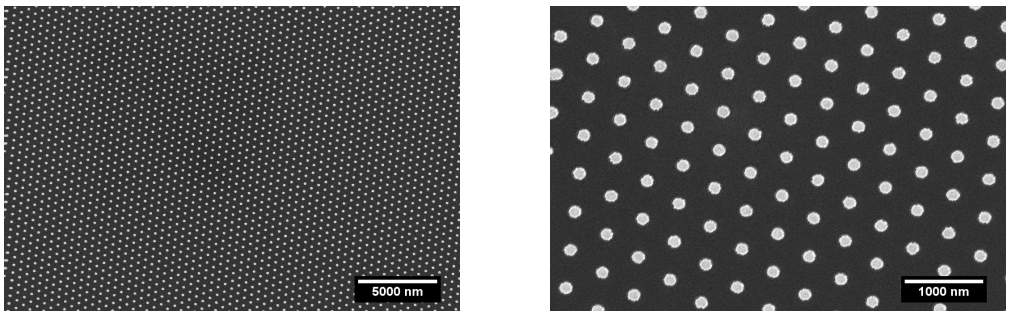

(a) Overview *(b) Close-up*

Figure 3.3: Shows an area of wafer 2 with 153 nm seed particles after processing and ready for growth. Processing on the other wafers looked overall identical, and therefore only results of wafer 2 are shown here.

The holes in the SiN mask were everywhere on all wafers, so the pattern transfer seemed to have worked flawlessly. Over large areas we could observe that some single gold particles missing, potentially being removed during lift-off. Since only very few particles were missing it is not thought to affect the growth of the NWs.

Local defects of larger significance were discovered on wafer 1 and 3. The lift-off process showed not to have worked as desired, leaving areas of the wafers covered in gold, see figure 3.4.

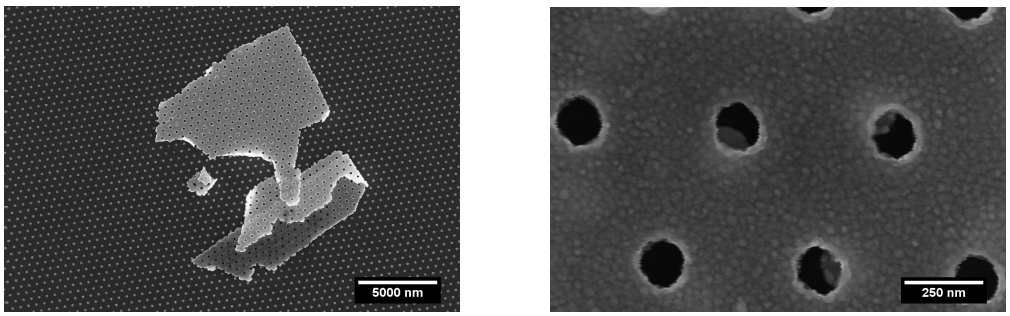

(a) Overview *(b) Close-up of the gold flake in (a)*

Figure 3.4: Shows top-view of wafer 1. These defects can be seen on the surface of wafer 1 and 3 after processing and over the whole wafers. The seed particles were 161 nm in diameter.

The areas covered in gold were several square micrometer large. These gold flakes were left on the substrates after processing and could not be removed by sonication. These gold flakes, even if only being local defects, could vastly affect the growth on these substrates.

It is not clear why the processing gave worse results on wafer 1 and 3 compared to wafer 2. On wafer 2 there was an error during spin-coating of the deep-UV resist layer. Causing the program to run for 35 seconds, then stopping, to then run again for another 10 seconds. Even though the total run time of the program was as desired, the final thickness of applied resist might have been altered by this. It could also be that, since a completely new bottle of resist was opened for wafer 1 and 3, a too thin layer was deposited, or that there were issues with the adhesion of the resist to the substrates, and therefore gold was deposited directly on the substrates due to resist missing in some areas. The wafers were however first investigated in SEM after finished processing, so the cause is not confirmed. Except the local defects, no further issues with processing on these wafers was detected.

To instigate the seed particle definition in more detail, higher magnifications images were taken and the cross-section was also analysed, see figure 3.5.

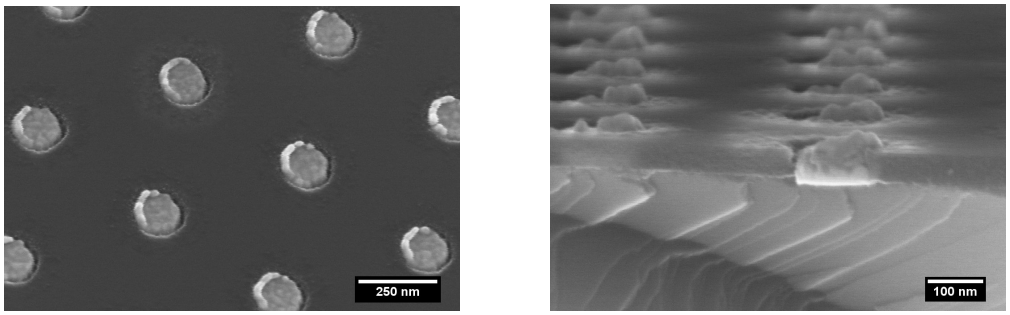

(a) Close-up *(b) Cross-section*

Figure 3.5: Shows close up images of wafer 3 from (a) top-view. (b) cross-section.

A ring-shaped shadow can also be seen around the holes of the mask in figure 3.5. This is probably a slight etching of the SiN mask that occurred during RIE, which is a very directional etch, but it seems to have affected the mask around the holes slightly. However this is not thought to affect the growth in any way.

Some of the gold seems to be deposited on top of the SiN mask, and some holes do not seem to be completely filled with gold. Overall the deposition seems not to be perfectly realized inside of the holes, which could lead to potential issues during growth.

Overall the substrates were not in perfect conditions for the growth, emphasizing that the processing needs optimization. It remains to be seen if any of these imperfections will have a significant effect on the NW growth.

3.3 Growth Optimization

All growth optimization was done on substrates from wafer 2. The growth optimization began by optimizing the GaP growth, starting from a previously known growth recipe. Thereafter the growth of the AlP NWs was optimized and lastly the axial AlP/GaP NW growth.

3.3.1 GaP NW Growth

InP Covered Reactor

We started the first growth experiments after an InP cover run, for reasons explained earlier. The first GaP growth, using a previously known growth recipe, resulted in very chaotic growth, as can be seen in figure 3.6.

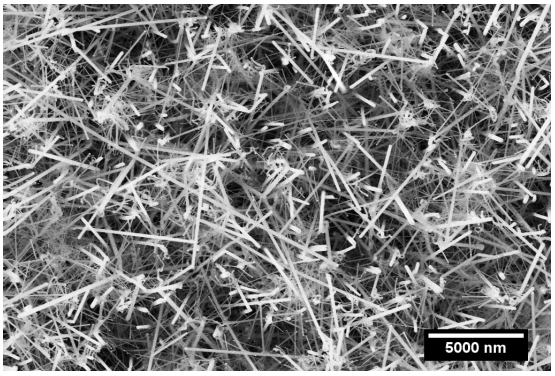

Figure 3.6: Shows a top-view of GaP NWs grown from a substrate from wafer 2 with 153 nm seed particles. Unoptimized growth parameters were used.

Since the growth looked as bad as in figure 3.6, it was speculated that the SiN mask had been affected by the high temperature annealing, which is a step in the growth recipes. This is usually used since it has been shown to enhance yield of growth for some materials, including GaP [42]. This high temperature annealing could potentially cause the SiN mask to delaminate from the GaP substrates due to the heating to high temperatures, introducing mechanical stresses between the interface of the materials due to thermal expansion mismatch of the layers [43, 44]. To investigate this, a sample was grown with the same growth conditions, but without the high temperature annealing step. This sample looked very similar to the previous sample, only slightly worse. This indicates that the high temperature annealing in fact has a positive effect on growth, or at least not worse. The high temperature annealing was therefore used in all further experiments. However, with this said, it will have to be further investigated if the mask adheres to substrate even after several runs in the reactor.

The effects of changing the molar fractions of the different precursors were investigated. After optimizing growth parameters, we grew substrates with 88 % yield at the center. The growth can be seen in image 3.7. The wires were 1.9 µm long, with an approximate growth rate of 380 nm/min. The length of the NWs could easily be adjusted by simply changing the growth time.

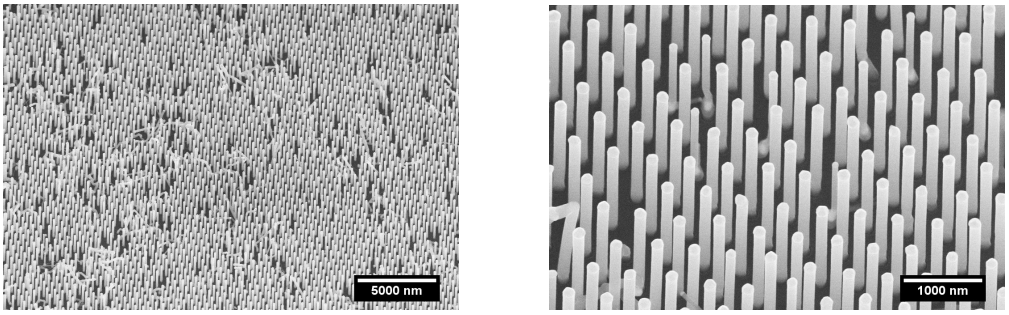

(a) Overview image *(b) Close-up image*

Figure 3.7: Shows the optimized growth of GaP NWs in an InP covered reactor. The substrate used was from wafer 2, with 153 nm seed particles. Images are taken with 30° *tilt.*

It can not be seen in the images, but the growth at the edges of the samples had a higher yield than at the center. This could be the case due to different conditions regarding temperature and V/III ratio at the edge compared to the center. It is likely that the growth is group-III limited for the phosphine rich growth conditions used, and therefore it is probable that there is a lower V/III ratio at the edge. This is due to that at the edge more group III-precursor can defuse to the substrate, since only a small amount of it will react and deposit on the susceptor. Once the material diffuses in towards the substrate it can react and contribute to material deposition at the edge.

That the growth is better at the edge strongly suggest that the growth recipes could be further optimized. However growth optimization is a time consuming effort, and since the yield was deemed sufficient for initial use and testing of the wires at AligND no further optimization was performed. Also, the optimal growth parameters might be different once GaP is grown on AlP, so it was avoided to spend to much time investigating the GaP growth.

GaP Covered Reactor

For GaP growth in an GaP covered reactor it was necessary to adjust the growth recipe again, due to the different conditions in the reactor. For reasons described later an In flush was introduced for growth inside a GaP covered liner, and growth without it was not investigated for GaP growth. With an increased background pressure of GaP in the reactor, compared to an InP covered liner, it was assumed that the molar fraction of TMGa should be decreased. However, in fact, the opposite showed to be true and a 40 % increase of the TMGa molar fraction showed best results. This could have to do with the changed properties of the alloyed seed particles, due to the introduced In flush.

With the new conditions in the reactor, GaP NWs could reliably be grown with a yield of 96 % at the center of the samples, see figure 3.8.

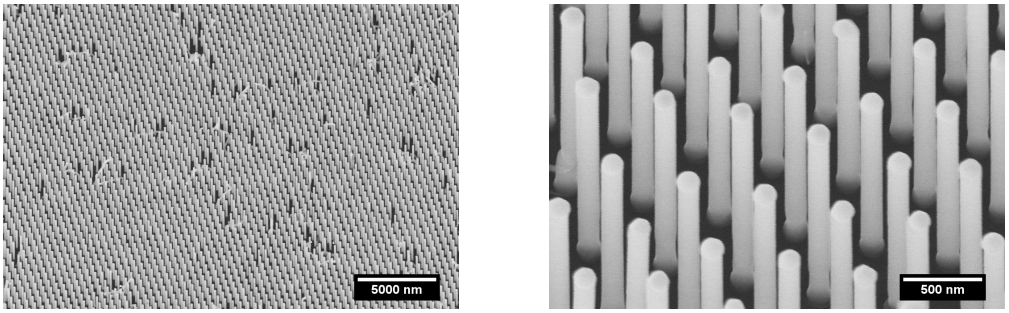

(a) Overview image *(b) Close-up image*

Figure 3.8: Shows the final optimized GaP growth in a GaP covered reactor with a yield of 96 %. The substrate used was from wafer 2 with a seed particle size of 153 nm.

With the the new conditions in the reactor the growth yield was 96 %, which is an improvement compared to when growing inside an InP covered reactor. The comparison is not completely fair since the GaP growth was not fully optimized for the InP covered reactor.

Full optimization of the GaP growth was also, in this case, not pursued, due to the reasons stated in the previous subsection.

3.3.2 AlP NW Growth

InP Covered Liner

First, an attempt was made to grow an AlP segment on top of a GaP NW, similar to the approach in R. J. Jams article [13], where they nucleated the substrate material first before growing the sacrificial layer.

The optimized growth recipe of GaP was run, and during the growth of the GaP segment the group-III precursors, TMGa and TMAl, were switched. For TMAl a molar fraction of approximately half of TMGa was used, since TMGa is a monomer [45] and TMAl is a dimer [46]. It was thought that this would result in roughly the same amount of material deposited, and was used as starting point for a growth recipe.

It showed to be possible to grow AlP segments with this approach. The wires, 0.95 µm GaP with 0.87 µm AlP on top, looked very similar to pure GaP growth, see figure 3.7, see figure 3.9.

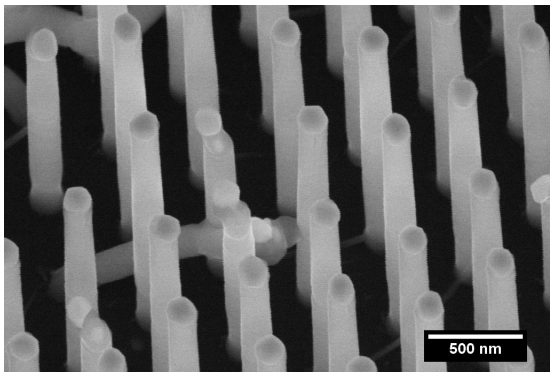

Figure 3.9: Shows GaP NWs with an AlP segment on top. The total NW length is 1.82 µm *of which 0.95* µm *is GaP and the remaining 0.87* µm *is AlP. The substrate is from wafer 2 with a seed particle size of 153 nm. Imaged at* 30° *tilt.*

By SEM inspection the AlP and GaP segment could not be distinguished clearly from the images taken, but by knowing the length of the previously characterized GaP segment and then measuring the final length of the NW after growth it could be concluded that AlP grew, and that it grew at a slightly slower rate compared to GaP, at approximately 217 nm/min.

Since the AlP grew nicely immediately on the first trial it was tested to nucleate AlP directly on the substrate with the same growth conditions for the AlP. The overall yield was high immediately, with 82 % of the wires standing upright at the center of the sample, see figure 3.10.

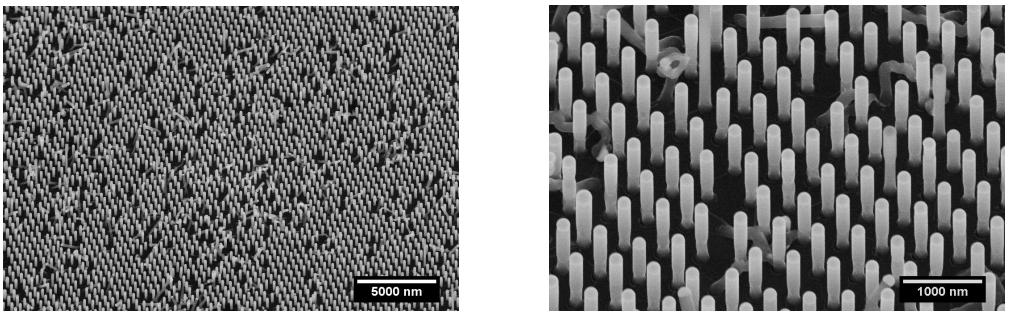

(a) Overview image *(b) Close-up image*

Figure 3.10: Shows the results of the first AlP NW growth. The yield was 82 % at the center. The substrate used was from wafer 2 with a seed particle size of 153 nm. Imaged at 30° *tilt.*

The NWs ended up being 1.1 μm long. The AlP grew with an approximate growth rate of 217 nm/min, the same rate as when grown on top of an GaP NW. For the AlP it was also found that the growth had a higher yield at the edge of the substrates, the same trend that was found when growing GaP.

After performing several experiments in an InP covered reactor there were issues with growing AlP NWs reliably. A trend was discovered that when the concentration of In in the reactor successively went down, after growing several samples, the yield and quality of the wires decreased until no wires grew at all. This required that we changed the approach used to grow AlP. The same trend was not observed for the GaP growth, this could be that the GaP growth is less sensitive to the amount of In in the gold seed particles, or that for these experiments the In amount in the reactor was fluctuating less.

With these results in mind it was clear that no AlP growth experiments could reliably be performed in a liner that previously had been covered with In, due to the background pressure of In fluctuating slightly and thereby affecting the growth for different runs. A different approach had to be used. Therefore, in all experiments that followed, a freshly etched liner was used and a GaP cover run was performed before beginning experiments. With this approach the background pressure of In in the reactor would be negligible and the growth would not be affected by it.

GaP Covered Liner

First a reference run was made, see figure 3.11. The same growth recipe was used as in figure 3.10. Again, the difference here being that the sample was grown after a GaP cover run in a freshly etched liner, meaning with no/negligible background pressure of In in the reactor.

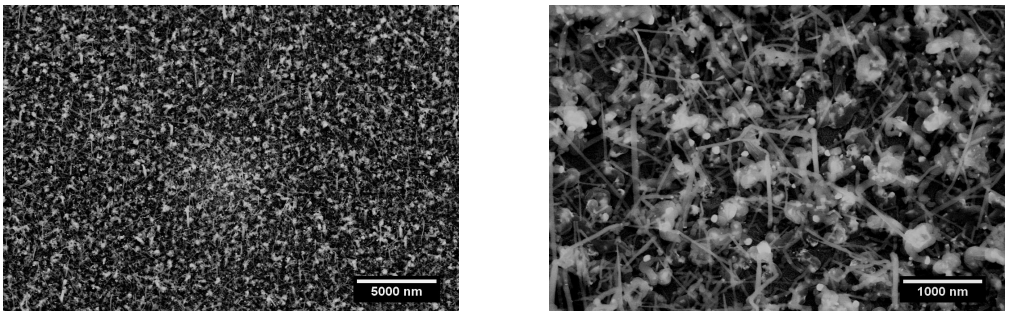

(a) Overview image *(b) Close-up image*

Figure 3.11: Shows the results of growing AlP in a GaP covered liner with a negligible background pressure of In. The same conditions as in figure 3.10 were used regarding substrate and growth recipe. Imaged at 30° *tilt.*

No growth of AlP could be observed, which was problematic. This meant that the growth would need to be re-investigated, perhaps in regards to different temperatures and/or other parameters. Also, since direct AlP nucleation on GaP has not been reported, it was not known if it would be possible to grow the NWs without In inside the seed particles. Instead, in order to save time, a low temperature Indium flush was introduced in the growth recipe, before the high temperature annealing. This was done to make the amount of In in the gold particles controlled and reproducible, thereby in turn making the AlP NW growth reliable. Since this step was required for the AlP growth it was also used for the GaP growth, since GaP would ultimately be grown on AlP. To find the best conditions for this In flush we investigated the effect of temperature and duration of the step.

First it was tested to introduce TMIn at temperatures of 260, 280, 300, 350 and 400 °C into the reactor before the high temperature annealing, at the beginning of the growth recipes. Theoretically there should be a sweet spot at 350°C where TMIn will pyrolyse effectively but not PH3, or at least not to the extent where growth would occur [47]. At lower temperatures TMIn should not pyrolyse enough and at higher temperatures there is a risk of growing some InP stub under the gold particle. For the results see figure 3.12.

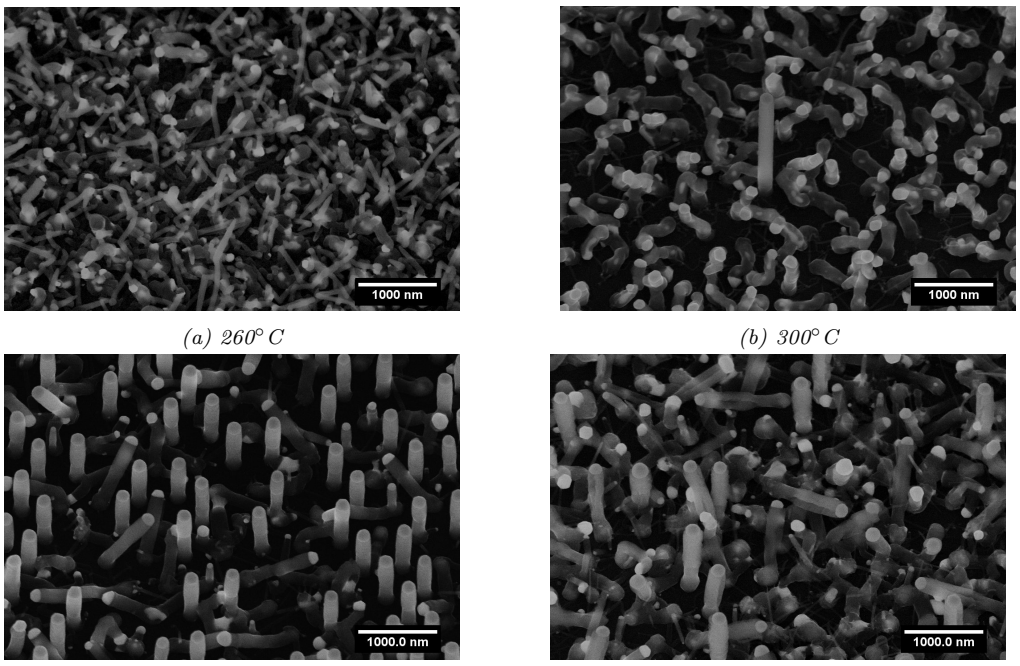

(a) 260° C *(b) 300° C*

(c) 350° C *(d) 400° C*

Figure 3.12: Shows the effect of the In flush on the AlP growth at different temperatures. The substrates were all from wafer 2 with 153 nm seed particles. The images are taken with 30° *tilt.*

It showed that, as predicted, the best result was obtained at 350 °C, which can be seen in figure 3.12. To further fine-tune the indium concentration in the seed particles, different durations of the flush were investigated, see figure 3.13.

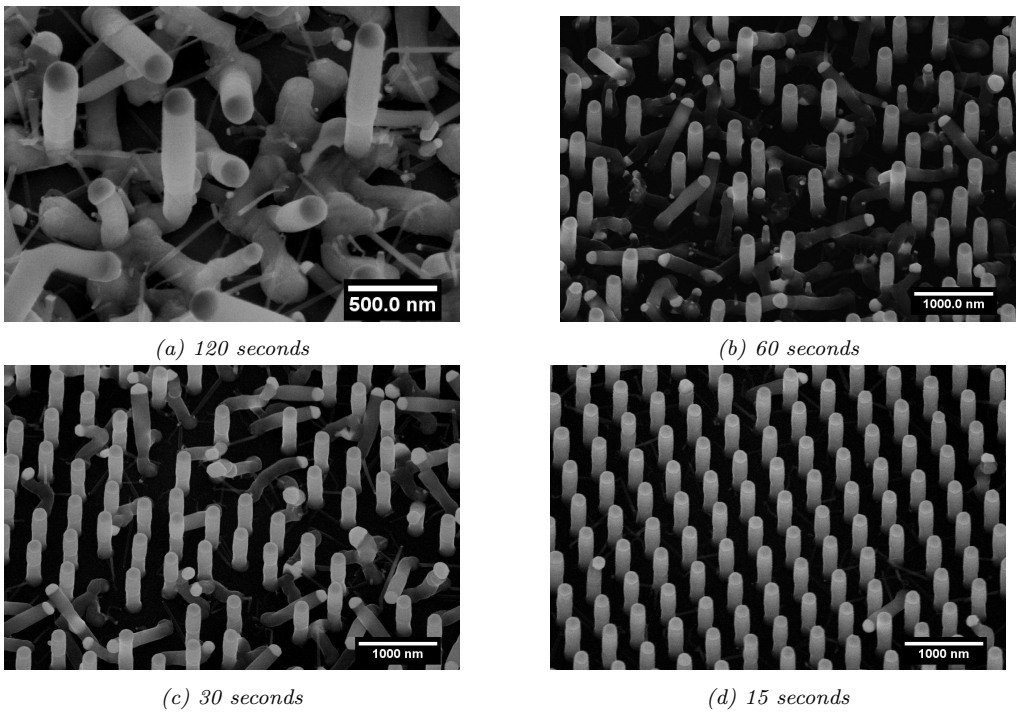

(a) 120 seconds

(b) 60 seconds

(c) 30 seconds

(d) 15 seconds

Figure 3.13: Shows the effect of the duration of the In flush on AlP NW growth. Substrates were from wafer 2 with a seed particle size of 153 nm. Note that the sample in (a) is imaged using a different SEM. All images are at the same magnification and at 30° *tilt.*

It showed to be favorable to only flush for a short time, as can be seen in figure 3.36d. The sharp time dependence clearly indicates that the growth of AlP is very sensitive to the amount of In in the gold particle. What exactly the role of the In is regarding the growth is still unclear to the scientific community. One might speculate that it changes the wetting angle, the saturation level of Al or the melting temperature of the alloyed gold particle. It could also perhaps catalyze chemical reactions, since In particles can be used as catalytic seed particles for NW growth [48, 49]. It could also be a combination of the alternatives listed above, or have some other unknown effect.

The yield of AlP growth combined with the optimized In flush showed to be very high at 96 %. The final results of the AlP growth can be seen in figure 3.14.

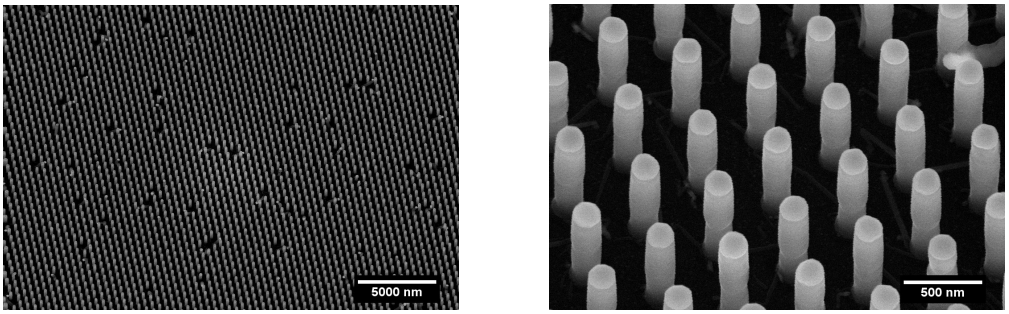

(a) Overview image *(b) Close-up image*

Figure 3.14: Shows the final optimized AlP growth with a success rate of 96 % on a substrate from wafer 2 with a seed particle size of 153 nm. Imaged at 30° *tilt.*

Many sections with perfect growth could indicate that the kinked NWs do not kink due to effects from the growth conditions, but rather that they might be affected by the, as previously discussed, not perfect seed particle definition and/or the SiN mask. Since this was still unclear, the effect of the mask was further investigated, which is discussed hereafter.

3.3.3 The Substrates Effect on Growth

To investigate the effect of the substrates, regarding the SiN mask and the seed particle definition, on the growth further, the two different seed particle sizes, 153 nm and 175 nm, on substrates of wafer 2 were compared. For a substrate with the larger, 175 nm, seed particles a HF dip was performed in the same way as before particle deposition (1:100, 23 °C, 10s). This dip was used to etch the SiN slightly, thereby opening the holes in the mask more. The growth could potentially benefit if the gold particles would no longer be in direct contact with the SiN mask. These three different samples were placed in the reactor for the same run. The same recipe as in figure 3.14 was used. Representable images of these samples can be seen in figure 3.15 below.

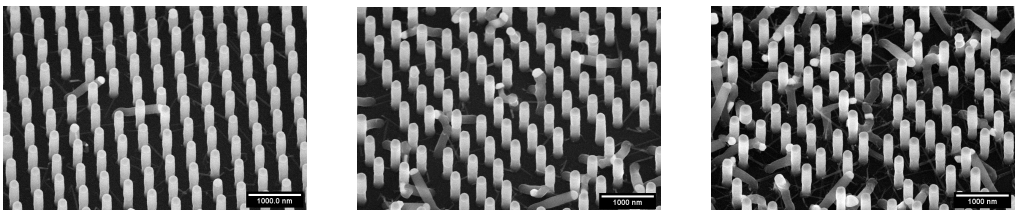

(a) 153 nm seed particles. *(b) 175 nm seed particles.* *(c) As (b) with HF-dipp.*

Figure 3.15: Shows representative images of differently prepared substrates from wafer 2 after they were exposed to the same NW growth recipe.

The small hole size gave the best results at 96 %, which is not surprising since the growth recipe was optimized for these particles. A worse result was seen for the large particles at 86 % and sample dipped in HF, which gave an overall worse result lowering the yield of the larger particles even further to 57 %. This hints at that the seed particle definition, and no the SiN mask, is affecting the growth negatively. As earlier mentioned the issue with the seed particle definition was that some gold was deposited on top of the SiN mask, and that the holes were not completely filled in some areas.

It was also found that similar substrates, used for growth in the same run could give samples with varying yield of the growth, indicating that different parts of the wafers gives a slightly different result. This could mean that the seed particle definition and/or the SiN mask are not completely homogeneous over the entire wafer. Completely homogeneous substrates at the nanoscale is always challenging to achieve at wafer level, but to see it affect the growth noticeable was not expected.

The Effect of HCl on AlP Growth

The effect of HCl on the AlP growth was also investigated, since it was necessary for the growth conditions used for GaP. It has been shown that HCl facilitates growth, and also reduces tapering of a variety of NWs, including GaP NWs [50]. For AlP the same molar fraction of HCl was used as for the GaP growth, which showed to have a very negative effect on the growth, see figure 3.16.

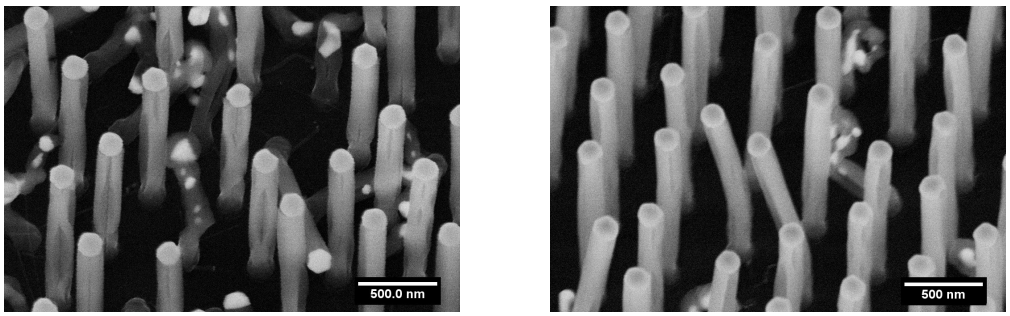

(a) From start. *(b) After 15 seconds of nucleation.*

Figure 3.16: Shows the effect of HCl on the AlP growth. The same growth and conditions as for the optimized AlP growth were used, figure 3.14. Imaged at 30° *tilt.*

The *in situ* etching with HCl at the molar fraction used for the GaP growth showed to etch the AlP too much during growth. The sidewalls of the NWs show large cracks in the material and the NWs have grown much more random than before. It showed to be more effective to nucleate the AlP first before introducing HCl, but the best approach showed to be to avoid the HCl completely for the AlP growth.

3.3.4 Axial AlP/GaP NW Growth

The previously found conditions for the AlP growth were used and combined with the growth recipe of GaP. All experiments were carried out in an GaP covered liner in combination with the developed In flush.

Interestingly, when growing GaP on AlP using a lower molar fraction of TMGa, the same as when growing in an In covered liner, gives a much better result compared to when using the GaP recipe that was optimized for the state of the reactor. Why this is the case is unclear, but it shows that the Al inside the gold seed particle changes the growth conditions for the GaP segment grown on top. Therefore the recipe had to be adjusted accordingly.

The most tricky part in growing AlP and GaP combined was the use of HCl. HCl was desired for the GaP growth, but as previously shown not for the AlP growth. It could not be used from start, since then the AlP growth then became failed, and also it could not be introduced at the same time as when switching group-III precursors, since nearly all wires kinked if this approach is was used. The best approach found was to start the HCl flow shortly before the precursors were switched. We found it to be optimal with a 15 second delay between introducing HCl and switching precursors.

Using the optimized growth recipe for AlP and GaP combined with the 15 second delay between introducing HCl and switching the group-III precursors we reliably grew samples as in figure 3.17.

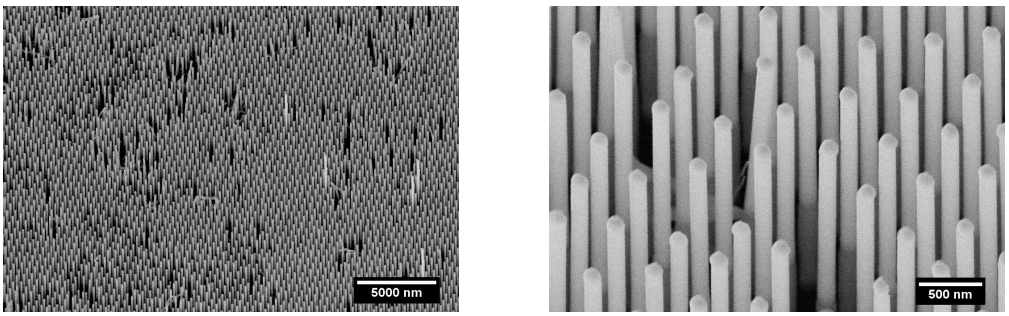

(a) Overview image *(b) Close-up image*

Figure 3.17: Shows the final optimized growth of axial AlP-GaP NWs on a substrate from wafer 2, with a seed particle size of 153 nm. The low contrast material at the NW base is AlP and the high contrast top segment is GaP. Imaged at 30° tilt.

With this approach 97 % of the NWs at the center of the samples grew as desired. We grew 1μm long AlP segments with 13μm long GaP segments on top, depending on what the NWs would be used for after removal from the substrate. The growth rate remained unchanged for GaP when growing on top of an AlP segment, at 380 nm/min.

To gain more insight on the interface between AlP and GaP, a cross-section analysis was done in SEM, see figure 3.18.

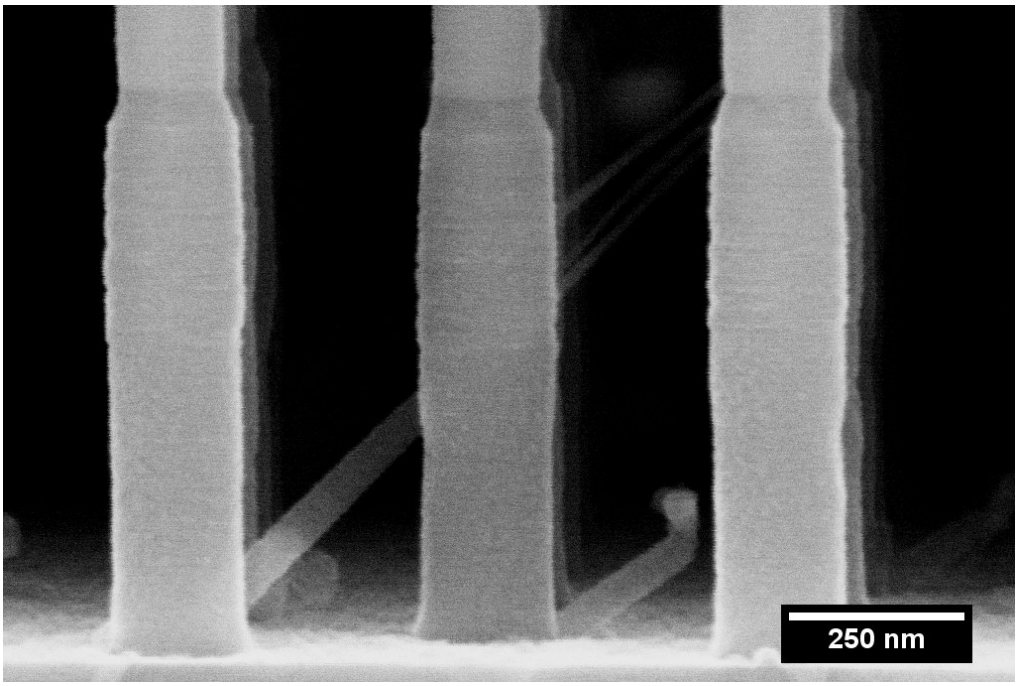

Figure 3.18: Shows a cross-section image of the interface between the AlP and GaP segment of axial AlP/GaP NWs. The low contrast material at the base is AlP and the high contrast material on top is GaP.

From the cross section analysis a clear, and strong effect of HCl on the wetting angle of the particle can be observed by the change in diameter of the NWs shortly before the interface of the AlP and GaP. This bottleneck shaped section represents the last 15 seconds of the AlP growth, where HCl is introduced. HCl increases the wetting angle which we found to be favorable for the GaP growth.

Some parasitic growth can also be seen in figure 3.18, which probably stems from, as previously discussed, gold on top of the SiN mask. This parasitic growth could affect the regrowth potential of substrates if it also occurs on substrates of wafer 1 used for the regrowth experiments. If the residues of the parasitic growth cant be removed it could lead to issues regarding regrowth.

With the growth optimized for AlP, GaP and AlP/GaP NWs the results are summarized in figure 3.19, which shows a side by side comparison of the different NWs in profile.

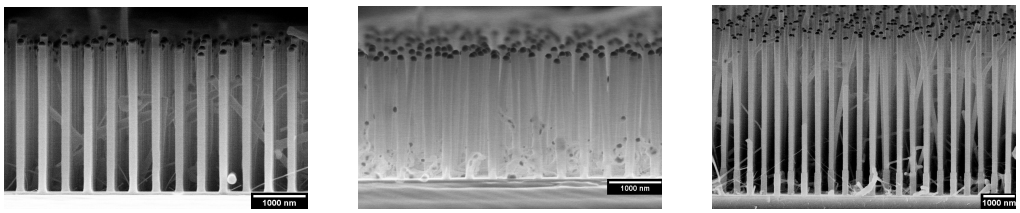

(a) GaP *(b) AlP* *(c) AlP/GaP*

Figure 3.19: Shows representative cross-section images of samples with GaP, AlP and axial AlP/GaP NWs, with a growth yield of 96 %, 96 % and 97 % respectively. Substrates were from wafer 2 with a seed particle size of 153 nm.

3.4 Etching Characterization

3.4.1 GaP Etch

To determine the etch rate of GaP NWs samples were prepared as described in section 3.3.1. The etchant used for all GaP experiments was diluted aqua regia, ($HCl : H_2O : HNO_3$, 3:3:2).

First a sample was etched at 45 °C for 30 seconds, see figure 3.1c. All samples described in this section were as in figure 3.20a before they were etched.

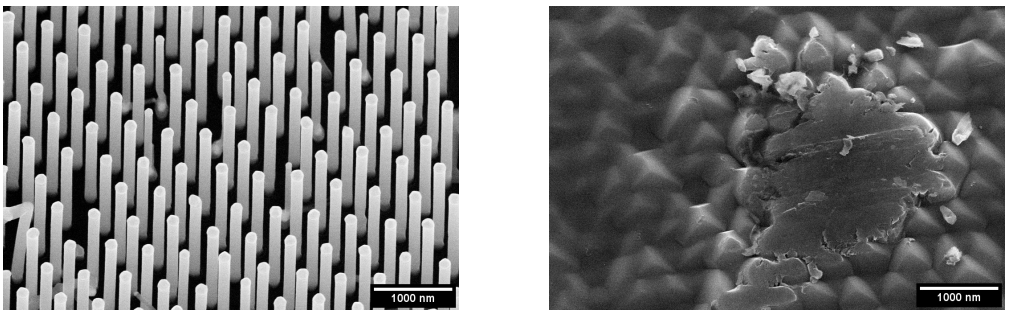

(a) Before Etching. *(b) After 30 seconds of etching.*

Figure 3.20: Shows a sample with GaP NWs before and after etching with aqua regia at 45 °C. Imaged at 30° tilt.

The etching at elevated temperatures showed a too high etch rate to be determined with this approach. All NWs were removed after 30 seconds by this etch. Even the SiN mask is etched by this solution, which is seen by the rough surface in figure 3.20b. Certain facets of the mask remain, and the holes seem still to have the same shape.

Since etching at elevated temperatures seemed to aggressive, the etchant was left to cool down to room temperature, 23 °C. New samples were then etched for 10 seconds and 30 seconds, see figure 3.21.

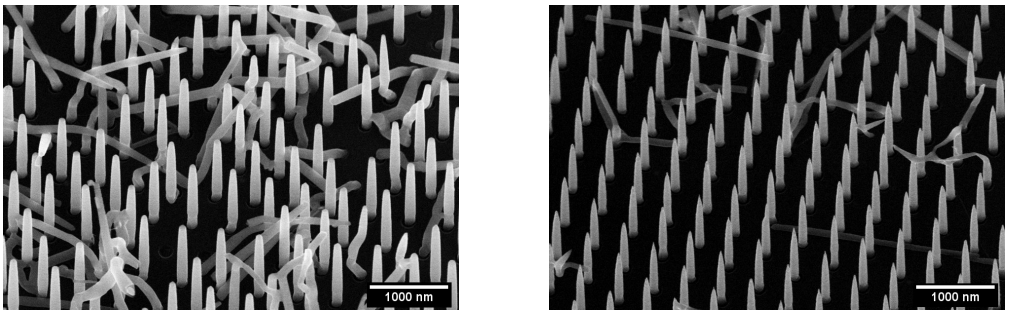

(a) After 10 seconds. *(b) After 30 seconds.*

Figure 3.21: Shows etching of GaP NWs with aqua regia at room temperature, 23 °C. Imaged at 30° tilt.

The gold seed particle seems to act catalytic for the etching, indicated by the strong tapering profile of the NWs after etching. Due to the strong tapering at the top of the wire the diameter measurements near the top are inaccurate and only the measurements of the lower half of the NW were used for determining the etch rate of the GaP NWs, which at 23 °C was 76.9 nm/s. The etch rate of Au was too high to be determined from these experiments, but has been shown to be 680 nm/min for a similar mixture of aqua regia ($HCl : H_2O : HNO_3$, 2:3:1, 30 °C) [51]. This regards etching

of Au deposited by evaporation, however of bulk and not of nanoparticles. We also do not have pure gold, rather a complex alloy of Au-In-Ga-Al-P, but it can be approximated that the seed particles etches at least 10× faster then the NWs.

The strong tapering and the ability of this etching process to remove the gold seed particle from the top of the NWs could be useful in some applications, such as photonics. It is common to remove the seed particles in further processing of the NWs, since it often is not desired for the final devices [52, 53]. The strong tapering observed has previously been reported on, where similar, cone like, shapes of NWs showed increased optical properties compared to conventional shapes [54, 55].

More experiments were carried out to investigate the etch further. We found that the etch rate was reduced by half if the etching solution never was heated, then being 34.4 nm/min. The etching profile, with tapering of the NWs, was the same as for the previous etch in figure 3.21. A trend was also discovered that the etch rate decreased over time, see figure 3.22.

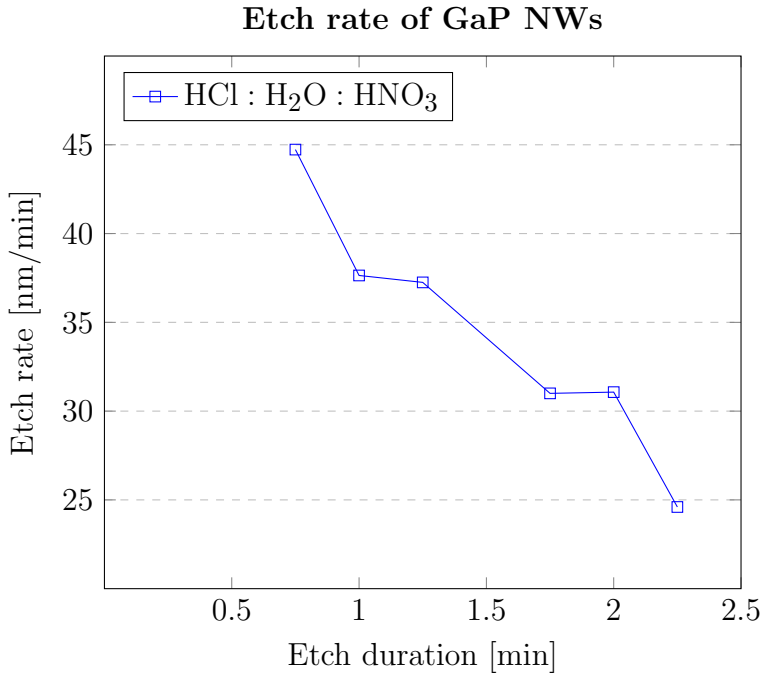

Figure 3.22: Shows a plot of the time dependence of the etch rate of GaP NWs etched by aqua regia (3:3:2, 23 °C).

The etch rate decreased with approximately 11.4 nm/min. What causes this reduction is unclear. One explanation could be that the etchant reacted at the surface and was not carried away, however the etching solution was stirred, therefore always fresh solution was provided to the solid/liquid interface. Another explanation could be that aqua regia loses its potency over time [56], but the experiments were performed in quick succession so this is most likely not the case either. Further research is required to explain this phenomenon.

When etching for 165 seconds, or longer, all NWs were completely removed and underetching of the substrates was evident, see figure 3.23.

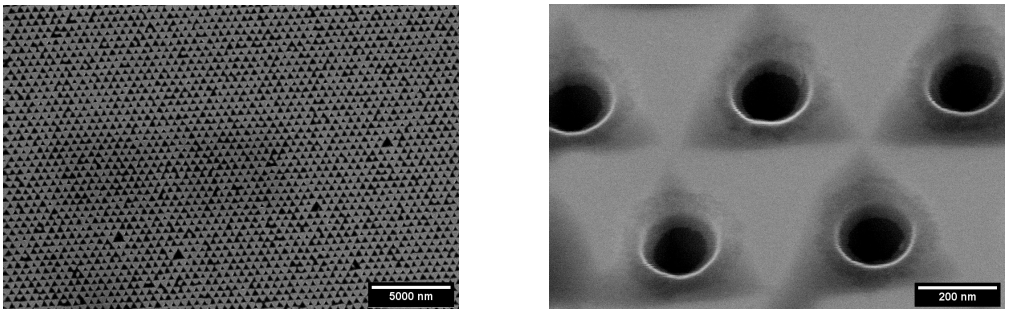

(a) Overview. *(b) Close-up.*

Figure 3.23: Shows the etching of NWs with aqua regia at room temperature, 23 °C, for 165 seconds. Imaged at 30° *tilt.*

The underetching is seen by the triangular shadows around the holes, below the SiN mask. The triangular shape comes from the etchant attacking (111)A planes while leaving (111)B planes, due to their difference in surface energy. These results also show that it would be difficult to reuse substrate with our approach if no selective etching would be used. We observed that either the NWs were not completely removed, or underetching of the substrate occurred, indicating that the etch process would have to be perfectly timed to flattening the surface in the holes.

3.4.2 AlP Etch

Before etching the samples grown on substrates from wafer 2 were again investigated in SEM. Two weeks had passed after growth and the samples had become heavily oxidised from being in air, see figure 3.24.

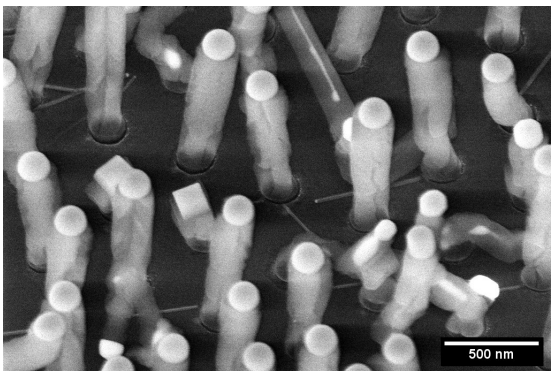

Figure 3.24: Shows AlP NWs, after the sample had been stored in air for 2 weeks. The NWs were heavily oxidized. Imaged at 30° tilt.

This oxidation was previously not discovered, since the samples were investigated in SEM immediately after growth. This phenomena could, after knowing about it, be observed already after 1-2 hours from the wires coming in contact with the oxygen and water in air. What exact material the NWs consist of after oxidation is unclear, it would need to be determined by material characterization. Such a characterization of oxidated AlP NWs has previously been done by M. T. Borgström et. al. [16], using Energy-dispersive X-ray spectroscopy (XEDS). Results showed that the material contained oxygen,phosphorous, and aluminum, but the exact composition was not determined. The oxidized AlP material could potentially be more chemical resistant than pure AlP, but this was not investigated since all NW were etched after being oxidised from being in air for a long time after growth.

Firstly it was investigated if the wires could be etched simply by submerging them in water, which showed no noticeable removal of material, even after 20 minutes. No efficient etch was observed for the mixture HCl:H2O at 1:100 either. The HCl mixtures at a ratio of 1:10 and 1:1 on the other hand showed to be potent enough to etch the AlP wires efficiently, however the wires did not etch homogeneously in all directions as the GaP wires did. The AlP wires etched mostly inside the large cracks of the NWs caused by the oxidation, and therefore no etch rate could be determined. For representative images of the NW etching see figure 3.25.

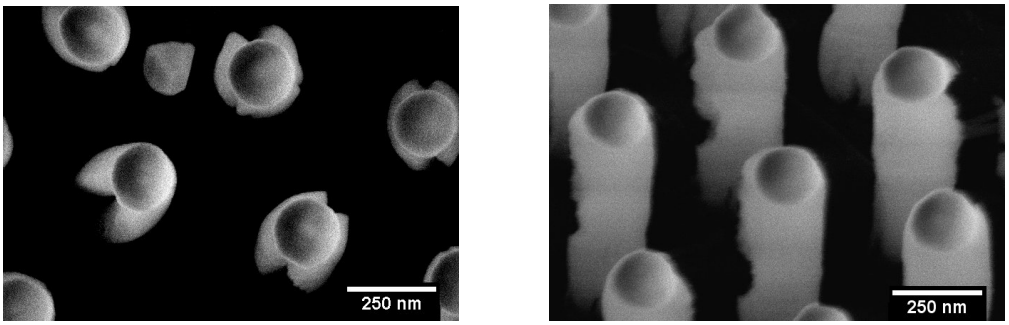

(a) Top-view. *(b) Side-view.*

Figure 3.25: Shows AlP NWs after being etched for 1 minute in $HCl : H_2O$ *at a ratio of 1:10 used. Imaged at* 30° *tilt.*

During imaging in SEM, gases were released from the samples. This was detected by increasing pressure in the SEM whenever oxidized AlP NW samples were loaded and illuminated by the electron beam. What gases were released is unclear, perhaps the NWs are releasing small amounts of phosphine. Regardless, the gases inside the SEM made imaging more difficult.

The etch rate is not of significance, since the interest in etching AlP lies in removing all of the material, and it being a material selective etch. Instead of investigating the etch of AlP NWs further it was proceeded with etching stubs of AlP left on substrates after sonication, for the regrowth experiments. Now only HCl mixtures of 1:10 and 1:1 were tested and later the piranha etch. The stronger HCl mixtures showed again to be potent enough to remove the AlP, see figure 3.26.

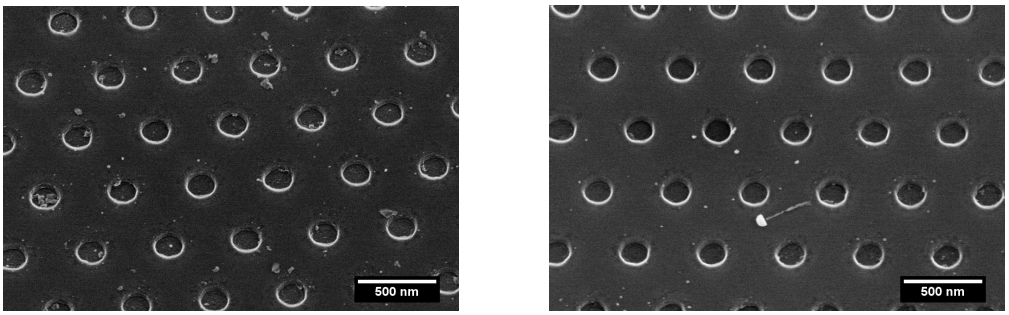

(a) 10 minute etch at a ratio of 1:10. *(b) 1 minute etch at a ratio of 1:1.*

Figure 3.26: Shows the sample surface after etching AlP stubs with the two most concentrated $HCl : H_2O$ *mixtures used. Imaged at* 30° *tilt.*

The more concentrated etch mixture, at a ratio of 1:1, gave an overall better result then the less concentrated mixture at 1:10. Less residues were detected when using the more concentrated solution, even when etching with the weaker solution for 10× longer. From SEM inspection the now exposed GaP surface in the holes of the SiN mask seemed to be clean and flat, as desired. It was also tested to etch a sample in the stronger solution for 5 minutes instead of 1 minute, but no noticeable changes could be detected using SEM analysis.

Next the diluted piranha etch was tested, see figure 3.27.

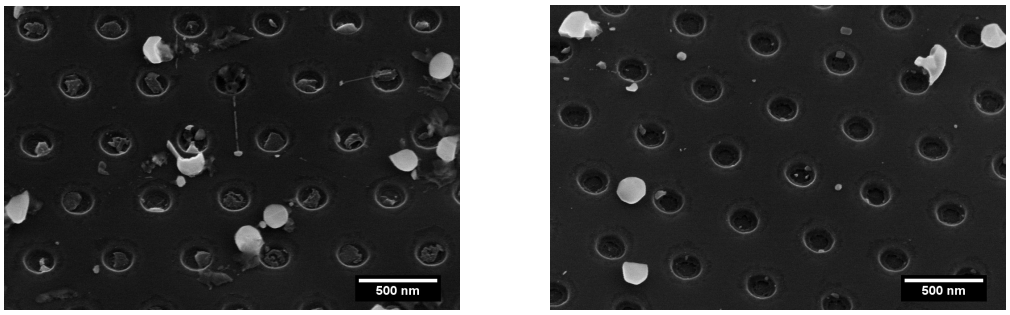

(a) 1 minute etch *(b) 5 minute etch*

Figure 3.27: Shows the sample surface after etching AlP stubs in diluted piranha solution. Imaged at 30° tilt.

The piranha etch does not remove AlP as efficiently as the HCl mixtures do. After one minute still a lot of residues remained in the holes and after 5 minutes the holes were still not completely clean.

From the results from this section the etch mixture for the substrate reuse experiments was chosen. The most suitable etch mixture showed to be $HCl : H_2O$ mixed at a ratio of 1:1. Since no apparent changes happened when etching substrates for longer durations than 1 minute, it was chosen to use this short duration to avoid potential issues with over-etching. Since we perform a selective etch over-etching should not be an issue, but exposing the samples to the least stressful environments is always preferable.

3.5 Substrate Reuse without Sacrificial Layer

As previously discussed, processing could be performed on wafer 3. It was unclear however if the rougher surface of this wafer would affect the epitaxial NW growth significantly. Wafer 3 was exclusively used for growth of GaP NWs for research purposes at AligND Systems.

The substrate was reused and GaP NWs could be grown at reduced yield, see figure 3.28.

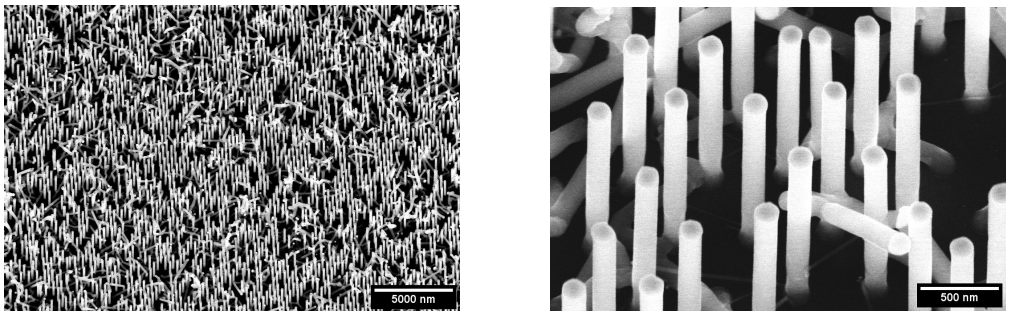

(a) Overview image *(b) Close-up*

Figure 3.28: Representative images of the GaP growth on substrates from wafer 3 with 161 nm seed particles. The growth had a yield of 50 %. Imaged at 30° *tilt.*

On average the samples from this wafer had a yield of 50 % at the center, which is quite low for pure GaP growth. Kinking was observed either immediately at the beginning of the NWs or not at all, indicating that the surface roughness causes the growth to be less optimal then on a perfectly smooth wafer.

3.6 Substrate Reuse with Sacrificial Layer

For the substrate reuse experiments 1×1 cm^2 substrates from wafer 1 were used. First AlP/GaP axial NWs were grown. Then the NWs were removed by sonication and residues of AlP were etched. Thereafter the samples were electroplated to redefine the gold seed particles and then exposed to growth again. Two cycles of regrowth were performed.

3.6.1 NW Growth

As a starting point for the growth on the substrates from wafer 1 the previously optimized growth recipe from section 3.3.4 was used. Surprisingly no epitaxial NW growth could be observed on these substrates using this approach. This was detected during growth with the use of the *in situ* measurements with LayTec, and therefore the growth of the GaP segment was skipped in the recipe. Representative images of the growth of the AlP segments can be seen in figure 3.29.

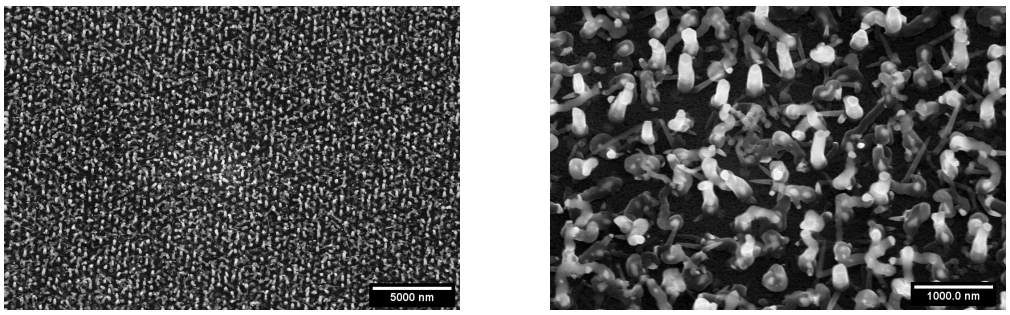

(a) Overview image *(b) Close-up*

Figure 3.29: Shows the surface of a substrate from wafer 1 after being exposed to the previously optimized growth recipe of axial AlP/GaP NWs. No epitaxial growth could be observed. Imaged at 30° *tilt.*

As discussed in section 3.3.2, the AlP growth showed to be very sensitive to the amount of In in the gold particle. Since only a small amount of TMIn was introduced into the reactor, it would be logical to assume that the amount of In was now lower in each gold seed particle on the new substrates, compared to the small substrates used for growth optimization. The amount of gold is not only higher due to the sample size and particle size being larger, but also the lift-off process was not perfect on substrates from wafer 1, as discussed in section 3.2. The substrates had gold flakes left on the substrate which were on the micrometer scale and probably collected a lot of the precursors, which further reduces the amount of In in the seed particles. An increase in duration of the In flush seemed necessary.

First the duration of the In flush was increased somewhat, and NW growth was observed at the edges of the substrates, suggesting that the amount of In in the particles at the center still was to low. The new optimum duration of the In flush was found to be 1:40 minutes for the 1×1 cm^2 substrates, which is a drastic increase from the 0:15 minutes previously used.

After that the In flush was adjusted a success rate of 80 % could be achieved. Representable images of the growth on the substrates can be seen figure 3.30.

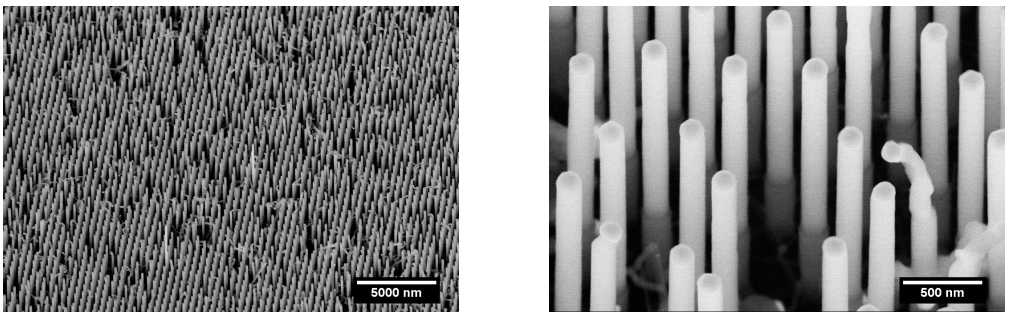

(a) Overview image *(b) Close-up*

Figure 3.30: Representative images of the AlP/GaP growth on $1 \times 1\ \mathrm{cm}^2$ *substrates with 161 nm seed particles. The growth had a yield of 80 %. Imaged at* 30° *tilt.*

It should be possible to achieve better growth with further optimization, but with limited amount of substrates to work with, and limited time, the growth recipe was not optimized further and was used on all remaining substrates.

With all things considered the success rate is still quite high, keeping in mind that the substrate had issues with processing, causing some areas to be covered with gold flakes. Residues of such a gold flake after growth can be seen in figure 3.31.

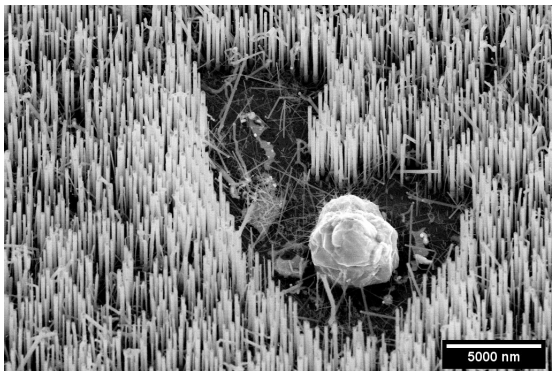

Figure 3.31: Shows a gold flake that melted into a clump after growth. Imaged with a 30° *tilt.*

Most of the gold flakes were gone after growth. In some cases they have melted together into small clumps. There were noticeable more flakes on the substrate before growth than clumps on the substrate surface after growth. How and if flakes were removed from the substrates is unclear.

3.6.2 Substrate Preparation for Regrowth

The substrate preparation before NWs could be grown from the substrate again were similar as in section 3.4.2. Here the NWs were harvested by AligND, involving a 10 minute sonication step, that mechanically removed the NWs and left stubs of AlP on the substrate, as in figure 3.32.

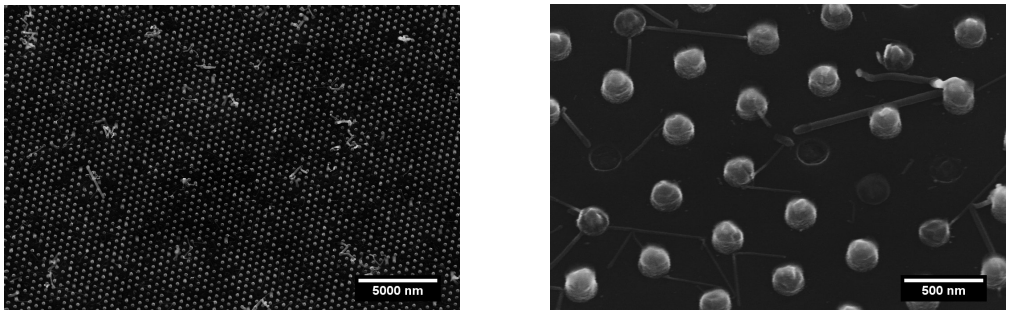

(a) Overview image *(b) Close-up*

Figure 3.32: Representative images of the substrates from wafer 1, after sonication. Clear residues of AlP can be seen in the holes of the SiN mask. Imaged at 30° *tilt.*

The substrate surface looked clean for the most part, with only AlP residues. In some areas there were still residues from parasitic growth and from NWs that crawled on the surface. What these residues are, AlP or GaP, is unclear but after etching they should be removed if it is AlP. These residues could later become issues regarding reuse, especially if they are inside or covering the holes in the SiN.

To remove the stubs the substrates were etched in $HCl : H_2O$ at a ratio of 1:1 for 1 minute, which was found in section 3.4.2 to be the best etch for AlP. After etching the substrates did not look completely clean, see figure 3.33.

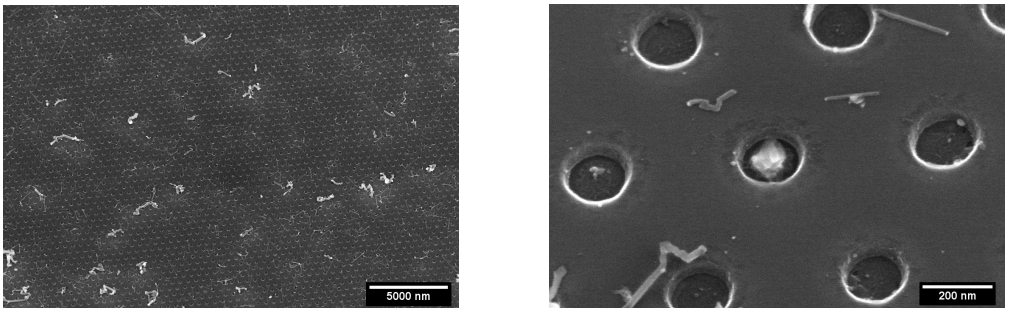

(a) Overview image *(b) Close-up*

Figure 3.33: Representative images of the substrate surface from wafer 1, after etching in $HCl : H_2O$ *for 1 minute. Clear residues of AlP can be seen in the holes of the SiN mask. Imaged at* $30°$ *tilt.*

To remove remaining residues the substrates were sonicated again for 10 minutes followed by one more minute of etching in the same solution. This gave better results, as in previously experienced on substrates used for etch characterization. Representative images of the substrates after the second etching step can be seen in figure 3.34.

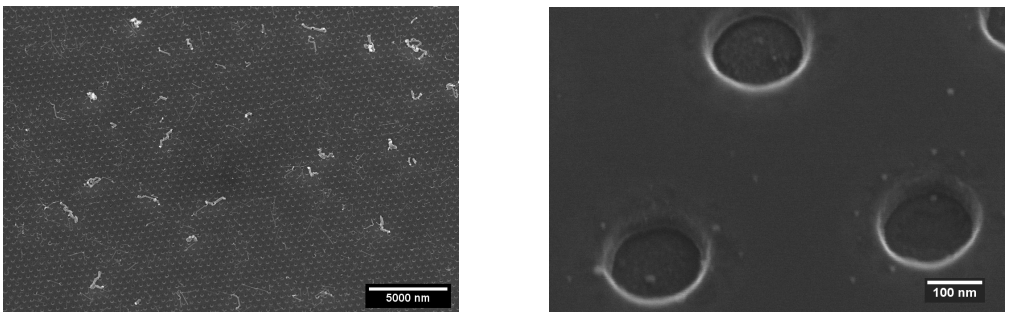

(a) Overview image *(b) Close-up*

Figure 3.34: Representative images of the the substrate surface after etching residues for 2 minutes in $HCl : H_2O$ *1:1. Imaged with a* $30°$ *tilt.*

In SEM inspection the substrates looked clean from residues, at least in the holes of the SiN mask. Some from parasitic growth and NWs that have bonded onto the substrates could potentially affect the regrowth. Since was not possible to remove these residues by etching it should be residues of GaP. The second sonication step might have helped a bit in removing these residues, but there are still many left. It is likely that these kind of residues can be avoided if the NW growth would be further optimized, making removal of the NWs easier and better processing, reducing the amount of parasitic growth.

It was proceeded with electroplating for seed particle definition, but first only on one substrate. The electrodeposition resulted in a very uneven deposition of gold, see figure 3.35.

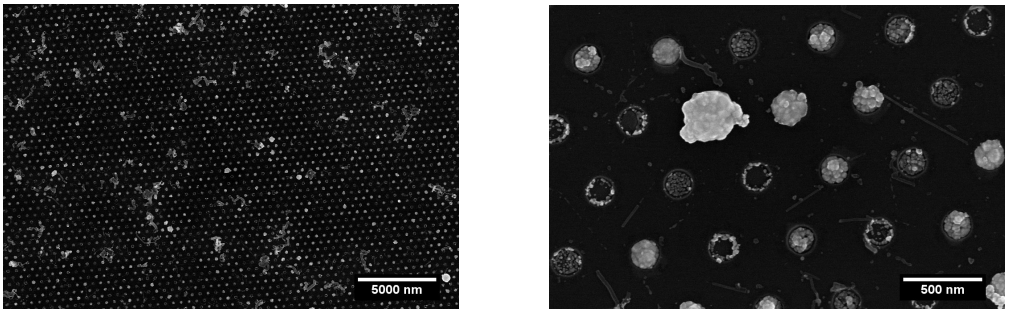

(a) Overview image *(b) Close-up*

Figure 3.35: Shows the first trial of electrodeposition. The substrate had been etched for 2 minutes in total. Imaged at 30° *tilt.*

Some holes were deposited with a lot of gold, while others had barely any deposition, indicating that there were still residues in the holes of the SiN mask. It could be a possibility that a thin layer of InP had formed during the low temperature nucleation or that some AlP residues are left and not visible in SEM.

Upon closer investigation of the SEM images a small shadow can be seen in some of the holes, as in the right hole in figure 3.34 previously shown. What these residues are can not be determined using simple SEM investigation, however it could be useful to investigate them to further the understanding of this process. Other techniques such as XEDS could be used to determine what material the residues are. To get a feeling for the amount of residues Atomic Force Microscopy could be used or investigating the cross-section of the substrate before deposition. However it was deemed too time consuming to investigate the samples with other techniques, and cross-section imaging in SEM requires to destroy a samples for further reuse since it needs to be cleaved. Instead it was chosen to remove any possible residues on the remaining substrates by further etching. The following etch times were tested; 5, 10, 15 and 20 minutes. Different durations were tested to find out how long time is needed to remove the residues from the holes without exposing the substrates to the etchant for a to long time. The effect of increased deposition cycles was also tested. For the results of the remaining samples, see figure 3.36.

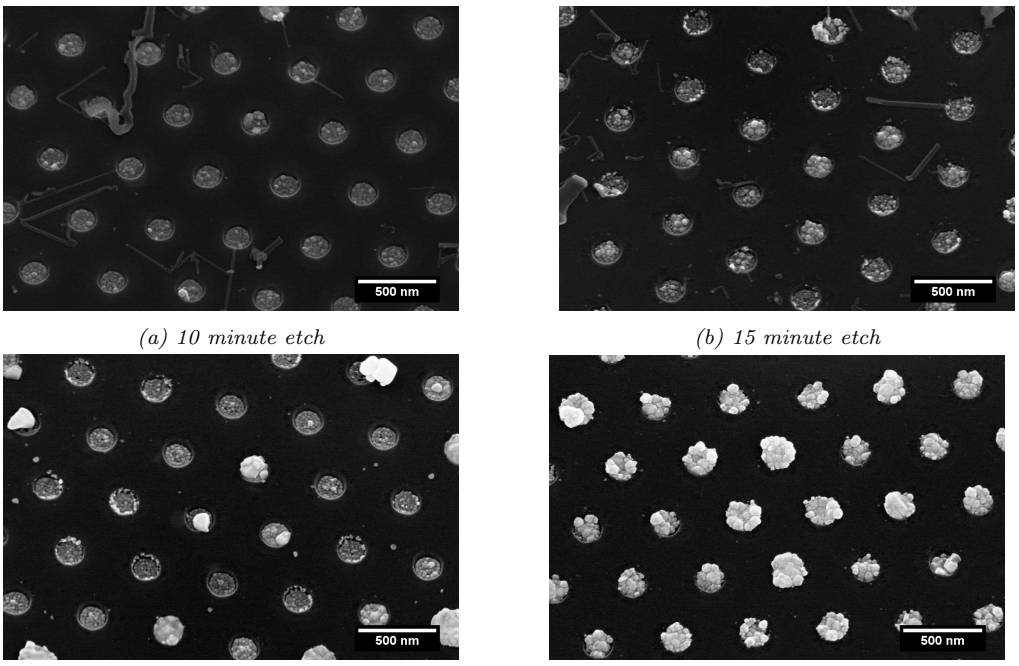

(a) 10 minute etch

(b) 15 minute etch

(c) 20 minute etch

(d) 20 minute etch with increased number of deposition cycles.

Figure 3.36: Shows the effect of the etch duration on the electrodeposition process as well as the effect of increased deposition cycles. Deposition cycles were set to 3500 (a-c) and 4200 (d). Imaged at 30° *tilt.*

Increased etch times did still not result in homogeneous deposition on the substrates. This indicates that these increased etch times still are to short or the etchant not being potent enough to remove all residues. It could also be that there is another unknown issue, limiting the deposition.

Increased deposition cycles resulted as planned in more gold deposited. If it is more desirable with the higher amount of gold or not will be investigated when growing the NWs.

The alternating amount of gold in different holes could lead to growth of wires with different diameters, and also affect the yield. Another problem could be that the In flush could be hard to adjust, since it is difficult to know how much gold is deposited on the substrates now compared to before when the particles were defined by evaporation. Also the amount of gold differs from substrate to substrate now, which further complicates the situation.

It can also be seen in figure 3.36 that the gold is deposited with a lot of small grains. This also indicates that the gold is not nucleating everywhere in the holes, probably due to residues. Locally the samples showed better gold deposition, such as in figure 3.37.

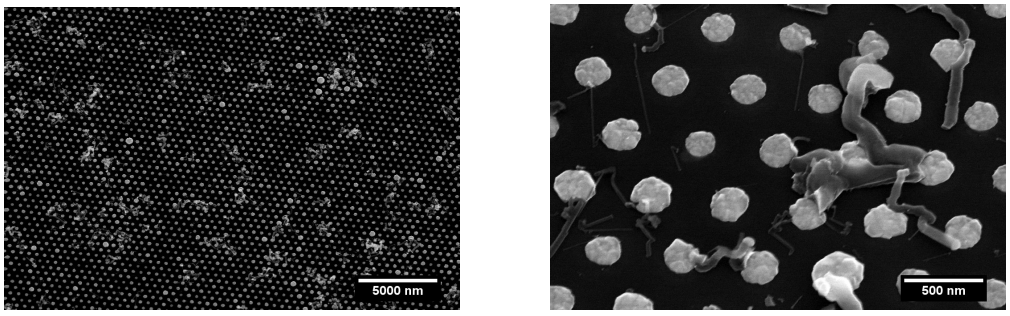

(a) Overview image *(b) Close-up*

Figure 3.37: Shows representative images of areas on the substrates which had better defined seed particles after electrodeposition. This occurred locally on the substrates. Imaged at 30° *tilt.*

Locally the substrates had nicely defined seed particles, being much less grainy and homogeneous. These local effects indicate that similar results are achievable on the entire substrates. Plausible reasons for local differences in deposition could be that the growth or the removal of the NWs might have been different in these areas.

3.6.3 Regrowth

For the regrowth on the substrates the seed particles were different since they were defined by electrodeposition. The samples were exposed to the same growth recipes as before, while adjusting the In flush for every sample due to varying amount of gold on different samples.

The first sample, from figure 3.35, was grown with a slight reduction in duration of the In flush, from 1:40 to 1:30 minutes. Barely any NWs grew from this sample, which looked very similar to samples where the In concentration was too high in the particle as in figure 3.36a. Due to these results, it was clear that further reductions of the duration of the In flush were necessary.

For the samples with a small amount of gold on them, samples a-c in figure 3.35, the In flush was set to approximately 30 seconds and for the sample with more deposited gold, sample d in figure 3.35, it was set to 1 minute. This is a significant reduction from 1:40 minutes used on the same substrates before electroplating, but so is also the amount of gold on the substrates.

For the substrates with a small amount of gold deposited, (a)-(c) in figure 3.36, regrowth was possible at reduced yield. As expected, there were many differently thick wires, as in figure 3.38.

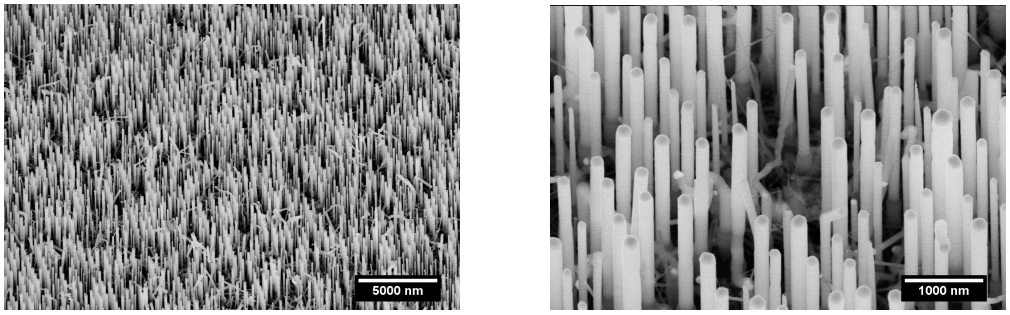

(a) Overview image *(b) Close-up*

Figure 3.38: Show representative images of the regrowth on samples a-c in figure 3.36. An average value for the yield of these samples was approximately 51 %. Imaged at 30° *tilt.*

These results were by no means perfect, but they do show that regrowth using the approach with a AlP sacrificial layer is possible. The ratio of standing wires and kinked wires was lowered for regrowth at approximately 51 % compared to 80 % before regrowth. The three substrates did not differ largely in yield, so slight increases of the etching durations did not seem to matter.

Comparison of the growth itself is not completely fair since; there was a lack of some seed particles and the holes were filled with a different amounts of gold, giving different growth conditions for some wires compared to others. Also the In flush could not be adjusted as well as before regrowth.

As discussed earlier, some areas of the samples had better defined seed particles. These areas also resulted in better growth, see figure 3.39.

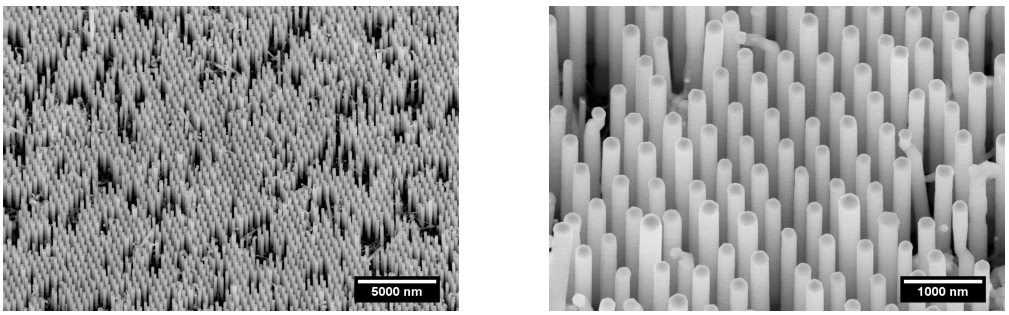

(a) Overview image *(b) Close-up*

Figure 3.39: Show representative images of the best areas of the samples in figure 3.38. Locally a higher yield was achieved, at approximately 62 %. Imaged with 30° *tilt.*

That better growth, now approximately 62 %, could be achieved locally suggests that the method can be optimized further. Achieving these results over the entire substrates.

A much better result was achieved on the substrate on which more gold was deposited by the increased amount of deposition cycles during electrodeposition, sample (d) in 3.35. The success rate was 81 % at most areas in the center and 87 % at the best areas. Due to more gold being in the holes of the SiN mask the growth was much more stable over the complete substrate, as in figure 3.40.

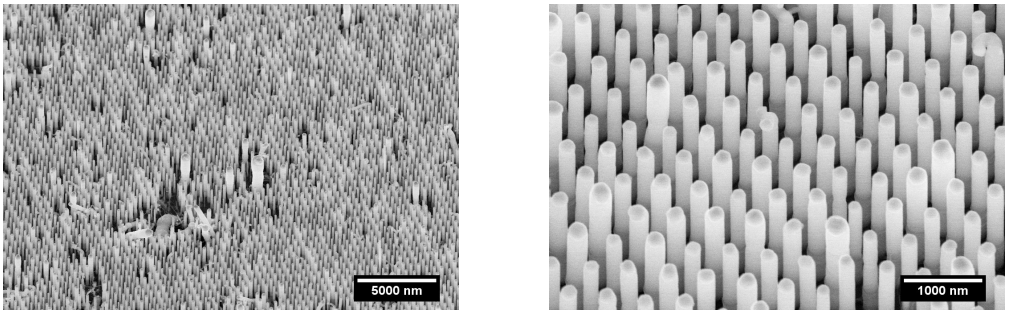

(a) Overview image *(b) Close-up*

Figure 3.40: Show representative images of the regrowth on sample d in figure 3.36, which had a higher amount of gold deposited on it. The yield was 81 % at the center of this substrate. Imaged at 30° *tilt.*

Increased gold deposition on this substrate led to a more stable NW growth and NW diameter. Some very large wires can be observed and those come probably from holes that were overfull with gold, indicating that we still have some issues with that some holes are cleaner than others.

For being the first experiments the yield was already high for the reuse, at least on the final sample. The most limiting part of the reuse process seemed to be the etching, which limited the seed particle definition by electroplating.

3.6.4 Second Reuse

The samples previously exposed to NW growth, removal and regrowth were reused again to see the effects of reusing substrates a second time. It was suspected, from the non homogeneous deposition with electroplating, that there might still be residues inside the holes of the SiN mask. In an attempt to improve the reuse process the samples were etched for longer times, 1 hour. Since the sample in the first reuse cycle with the most amount of Au deposited showed the best results the deposition cycles for electroplating were increased, from 3500 to 4200 for all substrates.

The same process as for the first reuse was repeated. The vastly increased etch time did not seem to have an effect, neither on the residues or negatively affecting the substrates in general, at least not visually when investigated in SEM, see figure 3.41.

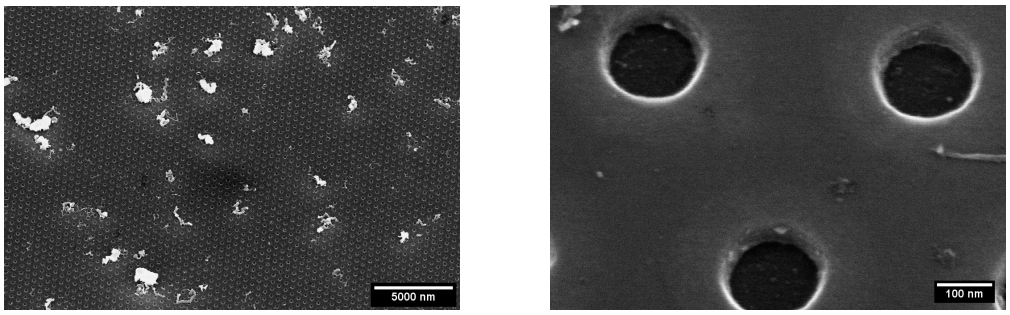

(a) Overview image *(b) Close-up*

Figure 3.41: Show representative images of the substrates after etching of the second reuse. Imaged at 30° tilt.

The substrate seemed to be in a similar condition as in the first reuse cycle. In some areas there was slightly more dirt on top of the SiN mask, but these residues did, at least for the first regrowth, not have a noticeable effect on growth.

The increased etch times did not seem to have the desired effect on the electroplating process, see figure 3.42.

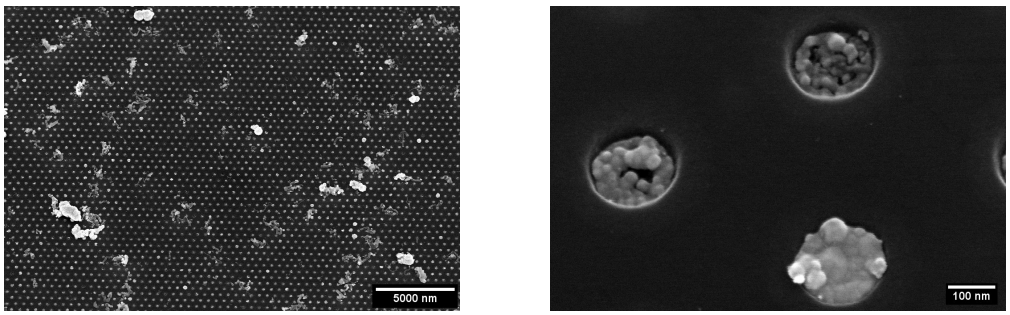

(a) Overview image *(b) Close-up*

Figure 3.42: Show representative images of the substrates after electroplating. Imaged at 30° tilt.

Even with the increased etch duration the substrates do not seem to be completely cleaned, since the electroplating still is not distributing the gold evenly over the substrate. Some holes contain more gold than others, also many holes have a grainy deposition which, as previously discussed, also is a sign of residues in the holes. Growing from these substrates a third time, the second regrowth, gave a similar result as previous growth. The yield was approximately 75 %. For representable images of the samples, see figure 3.43.

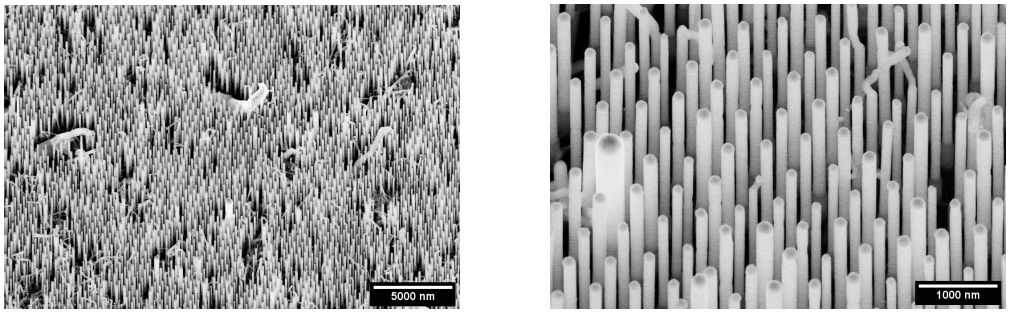

(a) Overview image *(b) Close-up*

Figure 3.43: Show representative images of the substrates after growth. The yield was approximately 75 %. Imaged at 30° tilt.

These results show that it is possible to reuse a substrate at least twice with the approach presented in this project. The second regrowth showed at slightly reduced yield, which could be due to more contaminations being on the SiN mask from the parasitic growth and GaP NWs that bonded to the surface. Similar to the first regrowth we see very large NWs growing and NWs with varying diameters.

The results show that the approach presented is viable, but needs optimization. We believe that with further optimization high yields and several cycles of reuse are possible. The substrates discussed were still intact after growing NWs three times from them, by reusing them twice, and it should be possible to reuse them further. We have shown that axial AlP/GaP NWs can be grown with 97 % using a SiN template mask and smaller seed particles. If starting with such a high yield on the substrates for reuse the substrates would probably have collected less contaminations for each reuse cycle, which would further the achieved reuse potential.

Chapter 4

Conclusions

We have demonstrated that GaP NW synthesis is possible at least three times from the same GaP substrates, by reusing the substrate twice with the approach presented in this work.

Three different types of NWs have been grown; GaP, AlP and axial AlP/GaP NWs with a yield of 96 %, 96 % and 97 % respectively. Such high yield was only achieved on the best substrates produced, which were from wafer 2 with 153 nm seed particles. Different yield was experienced on different substrates, even from the same wafers, indicating that processing still needs optimization to achieve more homogeneous results over 2" wafers.

Seed particle engineering with the use of an In flush allowed for direct nucleation of AlP NWs on GaP substrates. Without In in the seed particles no grow of AlP could be observed at 480 °C. The AlP growth showed to be very sensitive to the concentration of In in the Au seed particles while the GaP growth was not as sensitive.

Etch characterization of GaP NWs showed that their etch rate in diluted aqua regia, at room temperature, is approximately 34.4 nm/min. A trend was discovered that showed that the etch rate decreased linearly with etch duration, at approximately 11.4 nm/min. The same etch mixture was used for surface planarization of GaP stubs, left on wafer 3 from a previous standard GaP NW growth. Processing on this wafer could be performed as usual and epitaxial growth of GaP NWs was observed at reduced yield. The yield was low at 50 %, but nonetheless shows that substrate reuse also is possible using this approach. This approach showed to be less favorable than reuse with an AlP sacrificial layer, both in yield and in that it involves removal of the substrate material.

Of the investigated etch mixtures for AlP, concentrated HCl mixtures showed to etch it most efficiently. Submerging the AlP NWs in water or weak HCl mixtures resulted in no noticeable removal of material. The diluted piranha etch investigated removed large AlP segments fairly efficiently, but did not remove residues completely. It was not possible to determine an etch rate for the AlP NWs, due to non homogeneous etching of the NWs. The AlP NWs also showed to quickly oxidize in air, after approximately 1-2 hours the NWs were fully oxidized, which is thought to change their characteristics such as chemical resistance.

For the substrate reuse growth of axial AlP/GaP NWs was performed on 1×1 cm^2 substrates from wafer 1 with a seed particle size of 161 nm. A yield of 80 % was achieved for the first, conventional growth, while for the first regrowth a yield of 82 % could be achieved. For the second regrowth the yield was 75 %. The method is not fully optimized and can be improved in many areas. The method is showing high potential regarding substrate reuse and should be investigated further.

4.1 Outlook

The method proposed for substrate reuse still requires optimization. For example kinked NWs were sometimes not fully removed by sonication, and their GaP segment stuck to the substrate surfaces which resulted in increased sample contamination for each reuse cycle. All steps from processing and growth, to the reuse itself can likely be improved. The largest hindrance of this approach seems to be the removal of residues by selective chemical etching. To understand if, and what kind off residues are left in the holes of the SiN mask after etching requires more research. We propose two different approaches; either measure the amount of residues in the holes through a roughness measurement with an atomic force microscope, or to make a material characterization of the bottom of the holes, for example by using XEDS. Using either approach, or preferably both combined, would give much information on the morphology of the bottom of the holes.

To gain further insight into the effect and applications of alloying the seed particles with In further research is required. For example could be investigated if, and how, the wetting angle of the seed particles changes as a function of In concentration. Another approach could be to investigate the particles after the In flush and even to investigate complete wires in TEM. Another way could be to make a material analysis using XEDS to map the different materials in the NWs and gold particles to see where, and how much In accumulates.

It would also be interesting to revisit the AlP growth and attempt to grow AlP without the use of a In flush. This could be done by investigating different growth temperatures and molar fractions of precursors than investigated in this work. In case the residues in the holes are related to the In flush then this approach could improve the reuse process. Further this approach would make the NW growth more independent of substrate size and amount of Au in the reactor, which currently limits the growth.

It would have been a better approach to electroplate the wafers from start to be able to optimize the growth for seed particles deposited with this method, and to be able to make a better comparison between the first growth and the regrowth experiments. The process had however not been tested on GaP substrates in house, and therefore it was not an option to risk an entire 2" wafer, in case the process needed adjusting from known settings used for GaAs substrates.

A limitation of the electroplating set-up used was the holder for 1×1 cm^2 samples. For our experiments almost half of the substrates broke for every deposition cycle. With already a limited amount of substrates to work with this further limited the amount of experiments we could do. For the brittle GaP substrates a better holder would increase the ability to reliably investigate the effect of several cycles of reuse.

Further we would like to to suggest that the use of a sacrificial layer does not have to be limited to substrate reuse. It could perhaps also be used to remove gold seed particles from the top of NWs after growth, which can be desirable for certain NW applications. Other applications might also be possible when being creative. Further other material combinations, choice of sacrificial layers as well as etchants should be investigated to enhance the understanding and efficiency of such an approach.

Appendix A

Theory of processing techniques

A.1 Plasma-Enhanced Chemical Vapour Deposition

Plasma-Enhanced Chemical Vapour Deposition (PE-CVD) is a subgroup to CVD, a technique commonly used in nano and micro fabrication, to deposit a variety of materials as thin films and coatings. Such materials include carbon, silicon, carbides, nitrides, oxides etc. PE-CVD differs from standard CVD in that the energy for reactions is supplied by a plasma instead of by high temperature. [57, 58]

In PE-CVD gaseous precursors are introduced into a reaction chamber in which a plasma of an inert gas induces free radical formation and radical polymerization of the precursors, meaning the reaction energy is supplied by the plasma. Thereafter the reactive intermediates react further once they come in contact with the heated substrate surface . The chemical reactions at the surface cause nucleation of material, leading to film growth. By products released from the precursors during different reactions are gaseous and are removed by the gas flow through the reactor [58]. A schematic of the process can be seen in figure A.1.

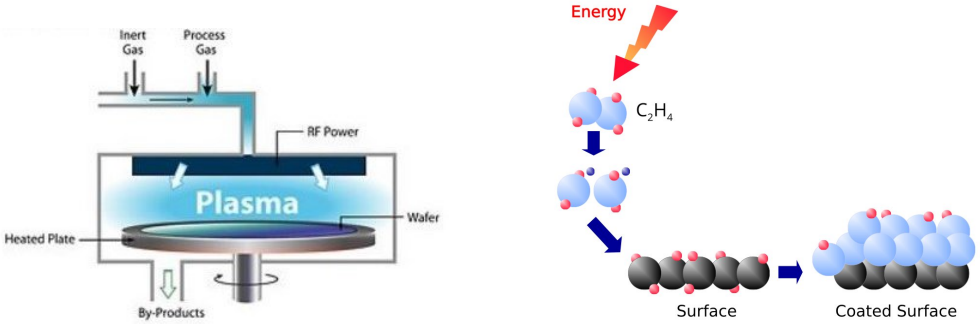

(a) PE-CVD system. Taken from [59]. *(b) Reactions in PE-CVD. Taken from[60].*

Figure A.1: Shows schematics of the PE-CVD process at the macro (a) and micro scale (b). A gas mixture of an inert gas and precursors are introduced into the reactor. The plasma causes the precursors to become reactive and deposit on the substrate. Note that (b) shows a Ethylene molecule, but the principle is similar for other molecules.

In this project PE-CVD is used for SiN growth, utilizing the reaction described below.

SiN layers are not chemically stoichiometric and are amorphous, therefore behaving differently than pure Si_3N_4. This is important since its material properties are chemically and structurally less stable, which affects etch characteristics and adhesion to other materials [61].

A.2 Displacement Talbot Lithography

Displacement Talbot lithography (DTL) is a new alternative to other lithographic techniques. It is a optical technique which utilizes the exposure of a photoresist through a photomask to transfer patterns. The light used for exposure is typically a monochromatic beam in the UV or deep-UV range. The technique offers high resolution pattern transfer over a large area while being flexible and scalable. [62, 63]

Talbot lithography utilizes the fact that light passing through a grating. due to constructive and destructive interference, it form self-images of the grating. This is called the Talbot effect. The self-images are present in a periodic interval, called a Talbot period. A Talbot pattern for a linear grating can be seen in figure A.2 below.

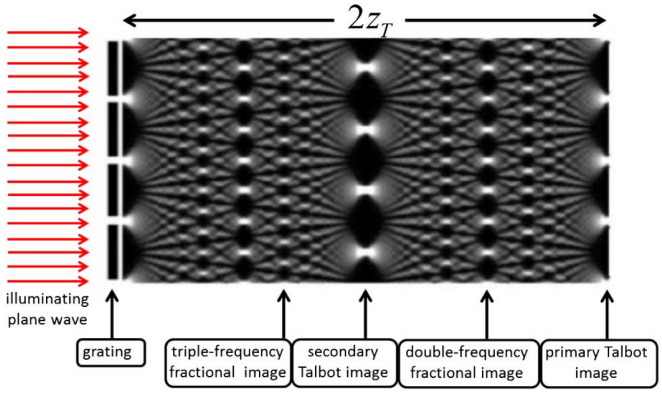

Figure A.2: Shows the Talbot effect for a linear grating that is illuminated by monochromatic light. Z_T *corresponds to one Talbot length and* $2 \times Z_T$ *is the distance between the grating and the primary Talbot image. Taken from [64].*

The distance from the grating to the primary Talbot image is given by $2 \times Z_T$ which corresponds to the primary Talbot length, where Z_T is one Talbot period. For a linear grating the Talbot period is determined by the grating period and the wavelength of light used for illumination. The relation is given in equation A.1 where Z_T is the length of one Talbot period, p is the grating period and λ is the wavelength of the light source. [64]

$$Z_T = \frac{2p^2}{\lambda} \tag{A.1}$$

The effective depth of field is very narrow when using conventional Talbot lithography, making good alignment of mask and substrate very difficult. This negative attribute is avoided when using DTL, where the sample is moved back and forth one Talbot period during exposure. [62, 63] This integration ensures that the whole range of lateral intensity distributions affect the exposure, thereby increasing depth of field and eliminating the need to place the wafer at a very precise distance from the mask. It also allows for patterning of samples that are uneven or coated with thick layers of photoresist. [62]

A.3 Reactive Ion Etching

Reactive Ion Etching (RIE) is a dry etching technique, based on a simple principle; a solid to be etched is affected by gaseous etchant producing volatile products that are gaseous and are removed from the substrate [65].

The gaseous etchants are typically different halogens. Other common gases used are are oxygen, hydrogen and nitrogen. For etching the gases are introduced into a reaction chamber, where they are excited and becoming a plasma of radicals and ions. The etching itself is then a process of ion bombardment, induced by an electric field, and chemically active species, both removing material. [65, 66] For a schematic, see figure A.3.

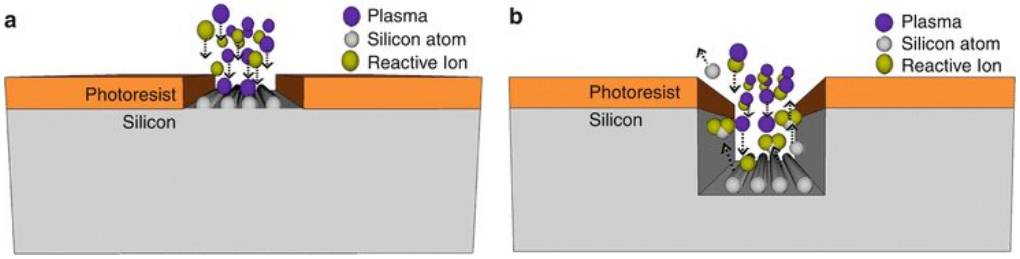

Figure A.3: Shows a schematic of the RIE process. Material is removed by selective etching of the substrate by ion bombardment and chemical reactions. Taken from [66].

RIE can, as wet chemical etching, be selective to etching of different materials. Materials that can be etched include different nitrides, oxides, carbides, metals etc. [65]. The advantage of using a dry etching technique, as RIE, compared to wet etching is that a much more anisotropic etch profile is achieved, which in combination of selective etching allows for patterning of small structures in nanoprocessing [67].

A.4 Thermal Evaporation

A classical approach to deposit materials, such as metals, in thin films or as in this case of seed particles for NW growth, is through thermal evaporation. It offers the ability to deposit high quality material with few impurities at a controlled deposition rate. It is a physical deposition technique in which material is heated until it evaporates and then condenses on a cold substrate.[68] A schematic of the process can be seen in figure A.4.

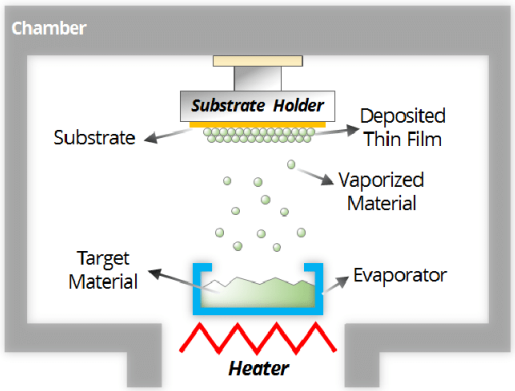

Figure A.4: Shows a schematic of the thermal evaporation process. The target material is heated until it is evaporating and condensing on the cold substrate. Taken from [69]

To ensure high quality of the deposited material, the deposition chamber is pumped down to low pressure, to reduce the risk of vapor molecules of the source material to collide with gas molecules. When the chamber is at low pressure the source material is heated above its melting temperature. Vaporized material will travel towards the substrate and once the vapor hits the cold substrate it will condense, thereby depositing a thin film of material. The vapor is traveling in a beam like fashion which allows for highly anisotropic deposition of material which is crucial for following nano and micro fabrication processing.[68]

A.5 Lift-Off

Lift-off is commonly used in combination with techniques such as Thermal Evaporation to control material deposition, such as metals, in nano- and micro fabrication [70]. ELO, a variant of lift-off, which can, as previously discussed, be used for substrate reuse. ELO involves highly selective etching of an epitaxially grown sacrificial layer to separate material from the substrate [71, 72]. Standard lift-off regards the removal of material by removing photoresist bellow[70]. The principle is the same for the two techniques; to remove material deposited on top of a layer that is removed by selective etching.

For illustration of the lift-off process we explain in detail how it can be used for seed particle definition for NW growth, see figure A.5 below.

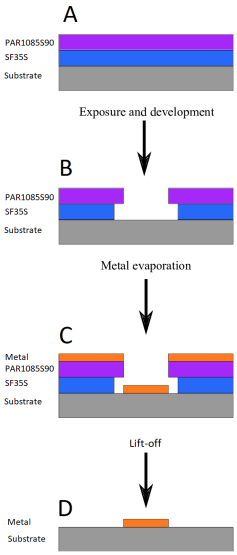

Figure A.5: Shows a schematic of the lift-off process, here used to define metal seed particles by metal evaporation. (A) After spin-coating. (B) After developing of resist. (C) After gold deposition. (D) After lift-off. Taken from [73].

Before any material is deposited on the wafer, the substrate is first coated with a double layer of photoresists. The resists are then patterned and developed. A double layer is used since it is desired to achieve an undercut shape, to avoid deposition on the sidewalls of the resists and to more easily etch the bottom resist, referred to as the lift-off resist. The target material is deposited on to the substrate using an anisotropic technique, such as thermal evaporation. After deposition the resist is removed and thereby also removing all excess material deposited on top of the resists. The removal of resist is the actual lift-off, separating the excess material from the substrate.

A.6 Pulsed Electrodeposition

Electrodeposition, also called electrochemical deposition, at the nanoscale is similar to conventional electrodeposition and pulsed electrodeposition differs only in the power supply used, described later. It can be used to deposit variety of different materials, such as metals, ceramics and polymers. Advantages of using electrodeposition to deposit these materials compared to more conventional techniques are many, such as; higher deposition rates, lower cost, the deposited material is free from porosity, many different substrates materials can be coated and more.[74]

Electrodeposition is based on oxidation-reduction reactions in a electrolyte. The electrolyte is a liquid in which metal ions are dissolved. These ions travel towards the cathode, the negative electrode, where they accept electrons and solidify. Thereby the process is depositing material on the electrolyte/metal interface. To coat a sample it has to be conductive and is placed in contact with the cathode, ideally covering it. The electrons for the reaction come from an external power supply. [75] A standard set-up can be seen in figure A.6.

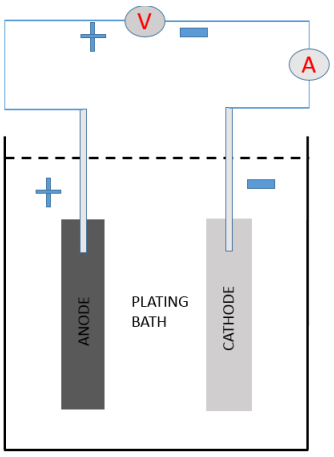

Figure A.6: Shows a schematic of the RIE process. Material is removed by selective etching of the substrate by ion bombardment and chemical reactions. Taken from [75]

In pulsed electrodeposition the signal from the power supply used can differ. Standard is to use square shaped pulses, the signal quickly varying between a zero and a non-zero value. The pulses are of equal amplitude, duration and polarity [75], see figure A.7.

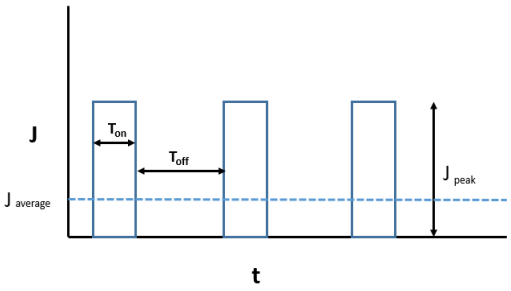

Figure A.7: Shows a standard shape of the signal from the power supply used in pulsed electrodeposition. The current density is denoted by J and time is reefed to as t. Taken from [75].

From the signal two important factors are the duty cycle and the average current density, see equations A.2 and A.3 [75].

$$\text{Dutycycle}(\%) = \frac{t_{on}}{t_{on} \times t_{off}} \tag{A.2}$$

$$J_{average} = J_{peak} \times \text{Dutycycle} \tag{A.3}$$

Material deposited with pulsed compared to standard electrodeposition is finer grained, has a more controlled microstructure and has overall better properties. This is due to the higher currents used which facilitates the nucleation process and that during the off-time adsorption, desorption and recrystallization can take place.[75]

Appendix B

Experimental Details

B.1 Substrate Preparation Before Processing

B.1.1 Substrate Cleaning

The cleaning procedure for wafer 2 was to place the wafer into a beaker filled with acetone, which was placed in a ultrasonic bath for 10 minutes. The wafer was then transferred to a beaker with isopropanol, which also was placed in a ultrasonic bath for 10 minutes. The wafer was then removed from the isopropanol and blow dried with a nitrogen gun. The cleaned wafer was thereafter placed in the sample box, ready for processing.

B.1.2 GaP Wafer Etch

The etchant investigated for the GaP etch was aqua regia. A mixture of H_2O : HCl : HNO_3 at 3:3:2 was prepared. After mixing the solution was left to rest for 15 minutes. For the etching at room temperature, 23 °C, wafer 2 was submerged in 100 ml of the etching solution. During etching the solution was slightly stirred. After 5 minutes the wafer was transferred to a large beaker with DI water which then was placed under flowing DI-water so that the beaker was overflowing. After SEM inspection the wafer was etched again in the same way. Lastly, after another visual inspection in SEM, the wafer was etched at 45 °C for 2 minutes. A hotplate was used for heating the solution.

B.2 Wafer Processing

B.2.1 Mask Deposition

The temperature of the heater in the reaction chamber was set to 250 °C which resulted in a temperature of 200 °C at the wafer surface. The RF power for the argon plasma was set to 300 W and the growth ran for 7 cycles, where every cycle had a duration of 20 seconds. The gas flows in the CVD reactor can be seen in table B.1.

Table B.1: Shows the flow rate for the various gases used in PE-CVD.

Gas Flows for PE-CVD	
Precursor	Flow rate (SCCM)
Argon	50
Silane	10
Ammonia	11.5

B.2.2 Lithography

It was ensured that no water or dust was on the wafer surfaces by blow drying the wafers with a nitrogen gun and then baking them at 200 °C on a hotplate for 10 minutes before lithography. After cooling to room temperature they were spin-coated with the bottom anti-reflection coating SF 3S, using an acceleration of 2500 RPM and a rotation speed of 2000 RPM for a duration of 45 seconds. Thereafter the wafers was again baked at 200 °C for 10 minutes and left to cool down to room temperature. The second resist layer was then applied by spin coating the wafers with the deep-UV resist PAR1085S90. Here the rotation speed was increased from 2000 to 4500 RPM, with the same acceleration as before. These are the same settings used when drying samples on the spin-coater, as an alternative to blow drying them with a nitrogen gun. After spin coating the wafers were again baked on a hotplate, now at 90 °C for 1 minute.

Before exposure of the deep-UV resist the Talbot was loaded with a dummy mask and dummy wafer to ensure good alignment between mask and sample. The dummy mask was then switched to a mask with a pattern of hexagonal holes that were 200 nm in size and had a 500 nm pitch. The dummy wafer was also changed to wafer 2, which was exposed first. For exposure the talbot system was configured as in table B.2.

Table B.2: Shows information about the DTL set-up used.

Talbot Setup	
Light Source Wavelength (nm)	193
Dose (mJ/cm^2)	3.0, 3.25 or 3.5
Frequency (Hz)	100
Separation (μm)	80
Talbot Distance (μm)	8
Polarization	None
Pulse Energy (mJ)	1.5
Power (μW/cm^2)	38

Wafer 2 was exposed with the doses 3.0 mJ/cm^2 on half of the substrate and the other halve was exposed with 3.5 mJ/cm^2. Next wafer 1 and 3 were exposed with a dose of 3.25 mJ/cm^2. After exposure of the resist the wafers were baked on a hotplate to set the resist. This was done at 100 °C for 50 seconds. After cooling down to room temperature the resist was developed by submerging the wafers into developer MF24A for 60 seconds. After developing of the resists the wafers were transferred to a beaker filled with DI-water. The wafers were left in the DI-water for 60 seconds and were then rinsed with softly flowing DI-water. The wafers were dried by running them on the spin coater with the same program used to apply the second layer of resist, with an acceleration of 2500 RPM and a rotation speed of 4500 RPM.

B.2.3 Pattern Transfer

To etch the SiN mask of a wafer, it was placed on a graphite carrier and loaded into the reaction chamber of the RIE system. Details in table B.3.

Table B.3: Shows the pressure, gas flows and RF-power used for the RIE process.

RIE	
Pressure (mTorr)	500
RF-Power (W)	75
CF_4 (sccm)	5
CHF_3 (sccm)	5
O_2 (sccm)	50

After RIE, the wafer was dipped in a diluted HF solution, HF:H2O at a ratio of 1:100, The wafer was dipped for a duration of 10 seconds and was then immediately transferred to a large beaker with DI water. This beaker was then placed under a stream of DI-water so that the beaker was overflowing. The wafer was left in the overflowing beaker for two minutes.

B.2.4 Seed Particle Deposition

The deposition rate of the evaporator was set to 2 Å/s which resulted in a actual deposition rate of 1.8 Å/s. The wafers were deposited with 65.3 nm of gold, measured by a quartz crystal microbalance.

For lift-off of excessive gold, the wafers were placed in a beaker with Remover 1165 that was heated on a hotplate set to 100 °C. The remover will remove both resist layers and thereby also the excess gold. To facilitate the lift-off, the beaker was alternatively moved from the hotplate to an ultrasonic bath with a bath temperature of 75 °C. The wafers were also lifted from the beaker and rinsed under flowing Remover 1165 to further try to speed up the process. After some time the remover in the beaker was replaced so that no loose gold was scratching the surface of the wafer during sonication. When all excess gold was removed from the wafers they were transferred to a large beaker with DI-water which then are placed under running DI-water for 2 minutes.

B.2.5 Wafer Dicing

To dice wafer 1 into pieces that would exactly fit the holder for the electroplating a Disco DAD 3320 dicer was used. Before the actual dicing the wafer was spin coated with a thick layer of resist, LOR 30B, to protect the nanopattern from being contaminated or damaged during dicing. The wafer was then glued onto a holder using UV curable dicing tape and placed inside the dicer. The dicer was programmed to yield 12 1×1 cm^2 pieces from the 2" wafer. After dicing the wafer was dried using a nitrogen gun and the dicing tape was exposed to UV light for 2 minutes. After exposure the diced pieces were removed from the dicing tape. To remove the thick layer of resist on the substrates and any residues of the dicing tape on the backside, all diced pieces were placed in remover 1165 for 1 hour at 80 °C. The pieces were then submerged and rinsed in DI-water followed by spin coating and baking on a hotplate for drying.

B.3 NW Growth Optimization

B.3.1 Etch and Cover run

The etch and cover run started with a flow of HCl at 750 °C for 60 minutes to assure that the liner and graphite susceptor were fully cleaned. After etching out the reactor an InP or alternatively a GaP dummy growth was performed, thereby covering the liner walls and the sucsceptor surface with the desired material. The InP dummy growth was done at 600 °C for 20 minutes and the GaP dummy growth at at 630 °C for 30 minutes. For details see table B.4.

Table B.4: Shows the temperature of the reactor and molar fractions of the precursors used during different steps of the etch and cover runs.

Etch and cover run						
Stage	**T (°C)**	**t (min)**	**χTMGa (a.u.)**	**χTMIn (a.u.)**	**χPH_3 (a.u.)**	**χHCl (a.u.)**
Etching	750	60:00	0	0	0	2.69×10^{-3}
GaP cover run	630	30:00	4.29×10^{-5}	0	3.85×10^{-3}	0
InP cover run	600	20:00	0	6.54×10^{-5}	6.92×10^{-3}	0

B.3.2 The Structure of the Growth Recipes

The growth recipes were started by heating the reactor, either up to 350 °C in the case of the In flush, or to 650 °C for the high temperature annealing. In either case, once the reactor temperature exceeded 300 °C the phosphine line was opened and was kept open until the reactor temperature dropped below 300 °C again, basically being open for the entire process.

For the In flush, which is an extra step used for growth in an GaP covered liner, the reactor temperature was stabilized at 350 °C for 2 minutes before TMIn was introduced by opening its line. The In amount of In that is dissolved in the seed particles is limited thermodynamically by the temperature used, and the amount of precursors available, controlled by the duration of the In flush. At the temperature used, 350 °C, the solubility was higher than needed for NW growth, and therefore the amount of In in the seed particles was controlled by adjusting the duration of the step. For our experiments typically varying between 15 seconds and 1:40 minutes, depending on sample size. The flush is terminated by closing the TMIn line and increasing the temperature of the reactor to 650 °C. After this extra step, the structure of the recipes were the same for the InP or GaP covered liners.

For the high temperature annealing the reactor temperature was set to 650 °C. Once the reactor temperature reached 650 °C the high temperature was held for 10 minutes for annealing under phosphine flow. After this annealing step the temperature was lowered to 480 °C, which was the growth temperature used.

Once the reactor reached the growth temperature of 480 °C a 2 minute temperature stabilization step was done, before the growth was initiated. To begin growth the lines of the desired precursors were opened and to stop growth the lines were closed again. The duration of the growth step determined the length of the NWs. Longer growth times result in longer NWs. We typically used 5-8 minutes, depending on the sample. To finalize the growth the heating of the reactor was switched off and the phosphine line was closed once the reactor temperature dropped bellow 300 °C.

B.3.3 Growth Recipes

GaP Growth Recipe

To grow GaP the following precursors were introduced into the reactor; TMGa, phosphine and HCl. For details on the molar fractions of the different precursors see table B.5. The molar fraction of TMGa is different depending on if the sample is grown in an InP or GaP covered reactor. In the case of a GaP covered liner the molar fraction was increased by 40 %, from 7.03×10^{-5} to 9.83×10^{-5} compared to when growing in an InP covered liner. As a reminder, the In flush is only used when growing in a GaP covered liner, otherwise this step is skipped.

Table B.5: Shows the parameters used for the GaP growth.

GaP Growth Recipe							
Stage	**T(°C)**	**t (min)**	**χTMGa (a.u.)**	**χTMAl (a.u.)**	**χTMIn (a.u.)**	**χPH_3 (a.u.)**	**χHCl (a.u.)**
In Flush	350	0:15-1:40	0	0	8.91×10^{-5}	6.92×10^{-3}	0
Annealing	650	10:00	0	0	0	2.31×10^{-2}	0
GaP Growth	480	5	7.03 or 9.83×10^{-5}	0	0	2.31×10^{-2}	1.85×10^{-4}

AlP Growth Recipe

The recipe is basically the same as for the GaP NWs except that the group-III precursor, TMGa, is substituted with TMAl and that no HCl is used. The molar fraction is also approximately halved since TMGa is a monomer [45] and TMAl is a dimer [46]. For the growth recipe see table B.6.

Table B.6: Shows the parameters for the AlP growth.

AlP Growth Recipe							
Stage	**T (°C)**	**t (min)**	**χTMGa (a.u.)**	**χTMAl (a.u.)**	**χTMIn (a.u.)**	**χPH_3 (a.u.)**	**χHCl (a.u.)**
In Flush	350	0:15-1:40	0	0	8.91×10^{-5}	6.92×10^{-3}	0
Annealing	650	10:00	0	0	0	2.31×10^{-2}	0
AlP Growth	480	5	0	3.48×10^{-5}	0	2.31×10^{-2}	0

AlP/GaP Hetero Growth Recipe

To grow GaP on AlP the recipes of AlP and GaP were combined. To switch from the growth of AlP to GaP the group-III precursors, TMAl and TMGa, are simply switched once the growth of the AlP segment is finished. A 15 second delay was used between introducing HCl and switching precursors, meaning that HCl was turned on for the last 15 seconds of the AlP growth. The growth recipe is summarised in table B.7.

Table B.7: Shows the parameters for the growth of the AlP/GaP hetero-NWs. It should be noted that HCl is introduced 15 seconds before the group-III precursors are switched.

AlP/GaP Growth Recipe							
Stage	**T (°C)**	**t (min)**	**χTMGa (a.u.)**	**χTMAl (a.u.)**	**χTMIn (a.u.)**	**χPH_3 (a.u.)**	**χHCl (a.u.)**
In Flush	350	0:15-1:40	0	0	8.91×10^{-5}	6.92×10^{-3}	0
Annealing	650	10:00	0	0	0	2.31×10^{-2}	0
AlP Growth	480	5:00-6:00	0	3.48×10^{-5}	0	2.31×10^{-2}	0
GaP Growth	480	5:00-8:00	7.03×10^{-5}	0	0	2.31×10^{-2}	1.85×10^{-4}

B.3.4 Growth Characterization

To characterize the growth the SEM images of the samples were analysed using the software ImageJ. To get a comparable value for the ratio of NWs that had grown straight compared to wires that had kinked, called yield, the automated contrast based algorithms of the software were used. Five top-view images were taken with SEM at randomly chosen areas of the sample, however either at the center or edge, at a magnification of 30k. The software was used to calculate the amount of straight wires per image. This data was then used to calculate straight NWs per area of this sample which then was compared to the theoretical value of the pattern, giving the ratio of standing and kinked wires.

B.4 Etch Characterization

B.4.1 GaP NW Etch

The etch solution was tested at the temperatures 23 °C and 45 °C. For high temperature only one duration was tested, 30 seconds. At room temperature different etch durations of 10, 30, 45, 60, 75, 90, 105, 120, 135, 165 and 195 seconds were tested.

To determine the etch rate the diameter of the NWs was measured before and after etching for every sample. This was done by imaging the NWs with SEM at 50k magnification and 30° tilt. The images were then analyzed in the software ImageJ, by measuring the diameter on 50 wires per sample. The diameter was measured on the top half as well as the lower half of each wire.

B.4.2 AlP Etch

Different etching solutions were tested in an attempt to return the substrate to its configuration before seed particle definition, by removing any residues in the holes of the SiN mask leaving a clean and flat GaP surface. The etching solutions tested were DI-water (H_2O), diluted HCl mixtures (HCl : H_2O at 1:100, 1:10 and 1:1) and also a diluted piranha etch (H_2SO_4 : H_2O_2 : H_2O at 1:1:5). The etch durations tested for the different solutions were one and five minutes. For DI-water and HCl mixtures also a 10 and 20 minute etch was investigated.

The first samples were etched by simply submerging them in the etching solutions to investigate the effect of the etch on the wires, and to get an idea of their etch rate in different solutions. After initial tests the etching was performed on samples where the wires first were mechanically removed by sonication, removing residues, such as stubs of AlP left on the substrate. All samples were characterized by SEM before and after etching.

B.5 Substrate Reuse

B.5.1 Etching

AligND harvested the GaP segment of the NWs with a process which included a 10 minute sonication step to remove the wires. The substrates were thereafter etched in HCl : H_2O 1:1 for 1 minute. After etching they were transferred to a large beaker with DI-water which then was placed

under flowing water for 2 minutes. After drying with a nitrogen gun they were exposed to another 10 minute sonication step in isopropanol. The samples were then etched further, but for different durations for different samples. Samples were etched for 2, 5, 10, 15 and 20 minutes in total.

For the second round of regrowth the substrates were etched for a much longer time, for 1 hour.

B.5.2 Electroplating

The electrolyte used for the gold deposition by electroplating is Gold Plating Services 24 K pure gold solution. For the experiments 160 ml of this solution was heated to 35 °C before deposition. The substrate was placed in a holder at a Au cathode. The cathode was placed at one end of the bath and a platinized titanium anode was placed at the other side of the bath. Between them a paddle agitator was installed which moved back and forth during deposition. The deposition was controlled by a signal generator, programmed as in table B.8.

Table B.8: Shows the settings of the signal generator that controls the Au deposition during electroplating.

Signal for Electroplating	
J peak (mA/cm^2)	6.8
Frequency (Hz)	20
Waveform	Square/Pulsed
Duty Cycle (%)	20
Duration (cycles)	3500 or 4200

After electroplating the samples were thoroughly rinsed under softly flowing DI-water and then dried using a nitrogen gun.

Lastly, before growth, the substrates were placed in an UV-Ozone cleaning system, FHR UVOH 150. The process lasted for 90 minutes, with the temperature set to 90 °C and the oxygen flow set to 500 sccm.

For the second cycle of regrowth the number of deposition cycles was set to 4200 on all the samples.

Bibliography

[1] T. W. Odom J. Hu and C. M. Lieber. "Chemistry and Physics in One Dimension: Synthesis and Properties of Nanowires and Nanotubes". In: *Accounts of Chemical Research* 32 (1999).

[2] Y. Xia et. al. "One-Dimensional Nanostructures: Synthesis, Characterization, and Applications". In: *Advanced Materials* 15 (2003).

[3] S. Barth et. al. "Synthesis and applications of one-dimensional semiconductors". In: *Progress in Material Science* 55 (2010).

[4] D. Gargas R. Yan and P. Yang. "Nanowire photonics". In: *Nature Photonics* 3 (2009).

[5] H. Unalan P. Hiralal and G. Amaratunga. "Nanowires for energy generation". In: *Nanotechnology* 23 (2012).

[6] F. Patolsky and C. M. Lieber. "Nanowire nanosensors". In: *Materials Today* 8 (2005).

[7] J.-P. Colinge et. al. "Nanowire transistors without junctions". In: *Nature nanotechnology* 5 (2010).

[8] P.C. McIntyre and A. Fontcuberta i Morral. "Semiconductor nanowires: to grow or not to grow?" In: *Materials Today Nano* 9 (2020).

[9] Enrique Barrigón et. al. "Synthesis and Applications of III–V Nanowires". In: *Chemical Reviews* 119 (2019).

[10] W. Metaferia et. al. "GaAsP Nanowires Grown by Aerotaxy". In: *Nano Letters* 16 (2016).

[11] M. Sugimoto M. Konagai and K. Takahshi. "High Efficiency GaAs Thin Film Solarcells by Peeled Film Technology". In: *Journal of Crystal Growth* 45 (1978).

[12] G. J. Bauhuis et. al. "Wafer reuse for repeated growt h of III–V solar cells". In: *Progress in Photovoltaics: Research and Applications* 18 (2010).

[13] R. J. Jam et. al. "Embedded sacrificial AlAs segments in GaAs nanowires for substrate reuse". In: *Nanotechnology* 31 (2020).

[14] W. Osten O. Madelung and U. Rössler. *Intrinsic Properties of Group IV Elements and III-V, II-VI and I-VII Compounds*. Berlin, Germany: Springer, 1987.

[15] M. Maedaa and K. Ikeda. "Stress evaluation of radio-frequency-biased plasma-enhanced chemical vapor deposited silicon nitride films". In: *Journal of Applied Physics* 83 (1998).

[16] M. T. Borgström et. al. "Fabrication and characterization of AlP-GaP core-shell nanowires". In: *Journal of Crystal Growth* 324 (2011).

[17] G. B. Stringfellow. *Organometallic Vapor-Phase Epitaxy Theory and Practice*. US: Academic Press, 1999.

[18] A. M. Gocalinska et. al. "Early stages of InP nanostructure formation on AlInAs". In: *Physical Rewiev B* 101 (2020).

[19] P. Ranga et. al. "Delta-doped beta-Ga2O3 thin films and beta-(Al0.26Ga0.74)(2)O-3/beta-Ga2O3 heterostructures grown by metalorganic vapor-phase epitaxy". In: *Applied Physics Express* 13 (2020).

[20] N. Goto et. al. "Characterizations of GaN nanowires and GaInN/GaN multi-quantum shells grown by MOVPE". In: *Japanese Journal of Applied Physics* 59 (2020).

[21] C. Blumberg et. al. "Spatially controlled VLS epitaxy of gallium arsenide nanowires on gallium nitride layers". In: *CrystEngComm* 22 (2020).

[22] S. Irvine and P. Capper. *Metalorganic Vapor Phase Epitaxy (MOVPE): Growth, Materials Properties, and Applications*. UK: John Wiley Sons, 2019.

[23] U. W. Pohl. *Epitaxy of Semiconductors*. Berlin, Germany: Springer, 2019.

[24] G. Cederberg R. M. Biefeld D. D. KoleskeJeffrey. *Handbook of Crystal Growth*. USA: Elsevier, 2015.

[25] S. Jalil. "Surface Chemistry and Electrical Properties of Nanowire Devices". PhD thesis. Linköping University, 2013.

[26] J. H. Lee H. S. Woo C. W. Na. "Design of Highly Selective Gas Sensors via Physicochemical Modification of Oxide Nanowires". In: *Sensors* 16 (2016).

[27] M. S. Dayeh A. Fontcuberta and C. Jagadish. *Semiconductor Nanowires I: Growth and Theory*. USA: Elsevier Science, 2015.

[28] M. Upmanyu N. Wang and A. Karma. "Phase-field model of vapor-liquid-solid nanowire growth". In: *Physical Review Materials* 2 (2018).

[29] E. Sutter et. al. “Axial Heterostructures with Phase-Controlled Metastable Segments via Post-Growth Reactions of Ge Nanowires”. In: *Chemistry of Materials* 31 (2019).

[30] D. V. Beznasyuk et. al. “Dislocation-free axial InAs-on-GaAs nanowires on silicon”. In: *Nanotechnology* 28 (2017).

[31] C. B. Maliakkal et. al. “In situ analysis of catalyst composition during gold catalyzed GaAs nanowire growth”. In: *Nature Communications* 10 (2019).

[32] N. Han et. al. “Controllable III–V nanowire growth via catalyst epitaxy”. In: *Journal of Materials Chemistry C* 5 (2017).

[33] M. T. Borgström. “In Situ Etching for Total Control Over Axial and Radial Nanowire Growth”. In: *Nano Research* 3 (2010).

[34] M. Heurlin et. al. “In Situ Characterization of Nanowire Dimensions and Growth Dynamics by Optical Reflectance”. In: *Nano Letters* 15 (2015).

[35] M. J. Madou. *From MEMS to Bio-MEMS and Bio-NEMS: Manufacturing Techniques and Applications*. USA: CRC Press, 2011.

[36] D. Biswas S. Tiku. *III-V integrated circuit fabrication technology*. USA: CRC Press, 2016.

[37] W. F. Waller. *Electronics Design Materials*. London, UK: Palgrave Macmillan, 1971.

[38] D. R. Vij. *Handbook of Electroluminescent Materials*. Routeledge: CRC Press, 2004.

[39] S. Adachi. *Physical Properties of III-V Semiconductor Compounds: InP, InAs, GaAs, GaP, InGaAs, and InGaAsP*. Canada: John Wiley Sons, 1992.

[40] M. Gad-el-Hak and T. Ebefors. *The MEMS handbook*. USA: CRC Press, 2002.

[41] M. T. Borgström et. al. “Synergetic nanowire growth”. In: *Nature Nanotech* 2 (2007).

[42] R. R. LaPierre J. Li. *Advances in III-V Semiconductor Nanowires and Nanodevices*. United Arab Emirates: Bentham Science, 2011.

[43] M. J. Madou. *Fundamentals of Microfabrication and Nanotechnology, Three-Volume Set*. USA: CRC Press, 2012.

[44] E. E. Gdoutos. *Fracture of Nano and Engineering Materials and Structures*. Dordrecht, Netherlands: Springer, 2006.

[45] C. A. LARSEN. “Decomposition Mechanisms of Trimethylgallium”. In: *Journal of Crystal Growth* 102 (1990).

[46] Z. Zhang et. al. “Experimental study of trimethyl aluminum decomposition”. In: *Journal of Crystal Growth* 473 (2017).

[47] S. Paiman et. al. “Growth temperature and V/III ratio effects on the morphology and crystal structure of InP nanowires”. In: *Applied Physics* 43 (2010).

[48] Z. He et. al. “A detailed study of kinking in indium-catalyzed silicon nanowires”. In: *CrystEngComm* 17 (2015).

[49] S. K. Chong et. al. “Synthesis of indium-catalyzed Si nanowires by hot-wire chemical vapor deposition”. In: *Materials Letters* 65 (2011).

[50] A. Berg et. al. “Growth and characterization of wurtzite GaP nanowires with control over axial and radial growth by use of HCl in-situ etching”. In: *Journal of Crystal Growth* 386 (2014).

[51] K. Gupta K. Williams and M. Wasilik. “Etch Rates for Micromachining Processing—Part II”. In: *Microelectromechanical Systems* 12 (2004).

[52] J. H. Woodruff et. al. “Vertically Oriented Germanium Nanowires Grown from Gold Colloids on Silicon Substrates and Subsequent Gold Removal”. In: *Nano Letters* 7 (2007).

[53] C. M. Hessel et. al. “Gold Seed Removal From the Tips of Silicon Nanorods”. In: *Nano Letters* 10 (2010).

[54] S. J. Gibson et. al. “Tapered InP nanowire arrays for efficient broadband high-speed single-photon detection”. In: *Nature Nanotechnology* 14 (2019).

[55] Y. Cui et. al. “Boosting Solar Cell Photovoltage via Nanophotonic Engineering”. In: *Nano Letters* 16 (2016).

[56] A. Collins. *Nanotechnology Cookbook*. UK: Elsevier Science, 2012.

[57] S. Neralla. *Chemical Vapor Deposition - Recent Advances and Applications in Optical, Solar Cells and Solid State Devices*. USA: IntechOpen, 2016.

[58] A. C. Jones and M. L. Hitchman. *Chemical Vapour Deposition: Precursors, Processes and Applications*. United Kingdom: RSC Publishing, 2009.

[59] Adhikaprasangi. *Methods of thin film preparation*. 2016, Retrieved: May 2020. URL: `https://pt.slideshare.net/anshukg/chemical-vapor-deposition-cvd`.

[60] Plasma Electronic GmbH. *Chemical Vapor Deposition (CVD)*. Retrieved: May 2020. URL: `https://www.plasma-electronics.com/chemical-vapor-deposition.html`.

[61] N. Jehanathan et. al. “Crystallization of silicon nitride thin films synthesized by plasma-enhanced chemical vapour deposition”. In: *Scripta Materialia* 8 (2007).

[62] F. Clube H. H. Solak C. Dais. “Displacement Talbot lithography: a new method for high-resolution patterning of large areas.” In: *Optics Express* 19 (2011), pp. 10686–10691.

[63] P.-M. Coulon et al. “Displacement Talbot lithography for nanoengineering of III-nitride materials”. In: *Microsystems Nanoengineering* 5 (2019).

[64] M. Xiao J. Wen Y. Zhang. “The Talbot effect: recent advances in classical optics, nonlinear optics, and quantum optics”. In: *Advances in Optics and Photonics* 5 (2013).

[65] D. Li. *Encyclopedia of Microfluidics and Nanofluidics*. Boston, USA: Springer, 2008.

[66] B. Bhushan. *Encyclopedia of Nanotechnology*. Dordrecht, Netherlands: Springer, 2012.

[67] P. J. French Y. X. Li and R. F. Wolffenbuttel. “Selective reactive ion etching of silicon nitride over silicon using CHF3 with N2 addition”. In: *Journal of Vacuum Science Technology B* 13 (2008).

[68] A. Lakhtakia R. J. Martín-Palma. *Engineered Biomimicry*. Pennsylvania State University, USA: Elsevier, 2013.

[69] S.-I. Park et. al. “A review on fabrication processes for electrochromic devices”. In: *International Journal of Precision Engineering and Manufacturing-Green Technology* 3 (2016).

[70] Z. Cui. *Nanofabrication: Principles, Capabilities and Limits*. United Kingdom: Springer, 2008.

[71] P. Demeester et. al. “Epitaxial lift-off and its applications”. In: *Semiconductor Science and Technology* 8 (1993).

[72] R. F. Leheny M. Dagenais and J. Crow. *Integrated Optoelectronics*. United Kingdom: Academic Press, 1995.

[73] V. Khayrudinov. “Towards single nanowire solar cell based on novel radial p-n junction”. PhD thesis. Aalto University, 2017.

[74] I. Gurrappa and L. Binder. “TOPICAL REVIEW: Electrodeposition of nanostructured coatings and their characterization—a review”. In: *Science and Technology of Advanced Materials* 9 (2008).

[75] M. Aliofkhazraei. *Electroplating of Nanostructures*. Tarbiat Modares University, Iran: IntechOpen, 2018.